Journal of Fusion Energy, Vol. 6, No. 1, 1987

Fusion Technology for a Magnetic Fusion Production Reactor[1]

R. B. Campbell,[2] D. L. Jassby,[3] and S. A. Freije[2]

The tandem mirror and tokamak are being considered as candidate fusion drivers for a materials production reactor that could be implemented in the 1990s. This report considers, in detail, the required performance characteristics of the fusion plasma and the major technological subsystems for each fusion driver. These performance characteristics are compared with the present state of the art, corresponding development needs are identified, and technology program requirements, in addition to those now being supported by the Department of Energy, are pointed out. The tandem mirror and tokamak fusion drivers are also compared with regard to their required advancements in plasma performance and technology development.

KEY WORDS: magnetic fusion production reactor; tritium production; fusion breeder.

1. INTRODUCTION

1.1. Background

Fusion reactors are being considered for the production of special nuclear materials because these reactors require no fissile feed, their production rate in atoms per unit thermal power can be several times higher than is the case in fission reactors, and they have the potential for much safer operation than is possible with fission reactors. Only magnetic confinement fusion (MCF) reactors are examined in this study. Of the wide variety of MCF concepts devised during the last three decades, only the tokamak (a toroidal device) and the tandem mirror (a linear device) are sufficiently well-developed and presently enjoy enough support to possibly form the basis of a production reactor in the late 1990s. Another paper[(1)] in this series details reasons for choosing the tokamak over other well-known toroidal concepts, as well as our reasons for choosing the particular tokamak embodiment that we have adopted as the basis of a production reactor.

Although fusion reactors have the potential for being substantially more attractive than fission reactors for materials production, fusion technology is at a comparatively rudimentary stage of development. In this paper, we are concerned only with the physics and technology requirements of the two candidate fusion drivers for a production reactor—the tandem mirror and tokamak—where *fusion driver* is defined as the fusion neutron source and the ancillary equipment needed to sustain that source. Other papers in this series are concerned with production blankets, reactor facilities, nuclear analysis, and the fuel cycle.

Figure 1 shows schematic trimetric views of the tandem mirror and tokamak production reactors (TMPRs and TPRs, respectively). While there is a notable difference between their linear and toroidal geometries, the fusion neutron source in both cases consists of a high-temperature deuterium–tritium (D–T) plasma contained in a vacuum vessel located in the bore of large circular or rectangular magnetic

[1] This paper represents work carried out from 1980 to 1982 and was in draft form in 1982. It was received for publication with only minor editing of its 1982 version, explaining the fact that some of the material is dated.

[2] TRW Corporation, Redondo Beach, California.

[3] Princeton Plasma Physics Laboratory, Princeton, New Jersey.

0164-0313/87/0300-0005$05.00/0

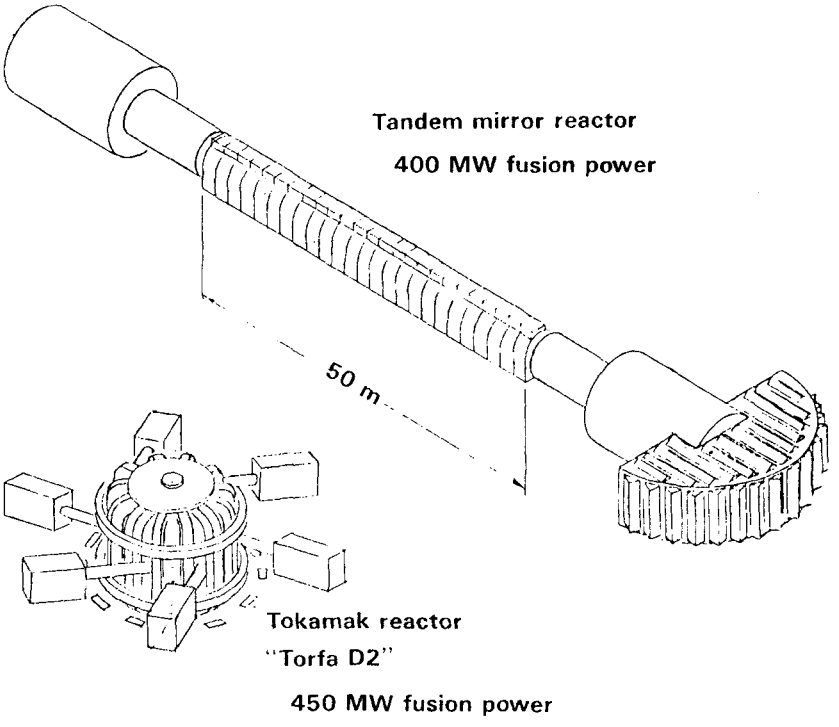

Fig. 1. Trimetric views of tandem mirror and tokamak production reactors.

coils. Both devices are supplied with auxiliary systems of comparable size for plasma heating, fueling, pumping, and tritium handling. Many of these subsystems are identical.

1.2. Study Objectives

This paper contains a preliminary assessment of the feasibility of using a tandem mirror or tokamak fusion neutron generator as the fusion driver of a materials production reactor. The two objectives of this study are:

1. To define the machine and plasma characteristics of suitable tandem mirror and tokamak drivers in sufficient detail so that the cost of materials production with either driver, using the production blankets described in Ref. 2, can be identified.
2. To identify the outstanding physics and technology uncertainties, as well as the required development programs, so that either fusion driver can be used in a materials production reactor to be operational in the late 1990s.

Materials production costs using these fusion drivers are not discussed in this paper.

1.3. Outline of Report

The next section of this paper describes the plasma physics features and major subsystems of the tandem mirror fusion driver. Two physics cases are presented: one reflects the plasma physics understood at the beginning of the study; the other, based on the latest tandem mirror physics, accounts for additional stability criteria. The plasma performance and characteristics required of the fusion technologies are compared with the present state of the art, and development needs are identified. These needs are then compared with those of existing development programs supported mainly by the Department of Energy Office of Fusion Energy (DOE/OFE), and additional program requirements are defined.

Section 3. of this paper contains an analogous discussion for the tokamak fusion driver. In Section 4. we compare the two candidate fusion drivers with regard to the advancements required in the plasma physics and fusion technologies to make each device

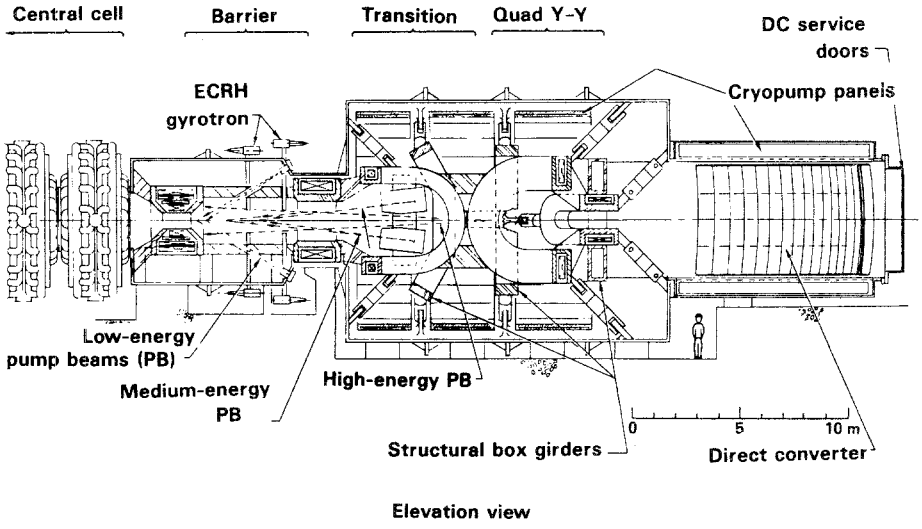

Fig. 2. End-cell configuration for the materials production reactor.

capable of serving as the basis for a materials production reactor. The last section presents our conclusions.

2. THE TANDEM MIRROR FUSION DRIVER

2.1. Plasma Physics Design Description

2.1.1. Baseline Design

The tandem mirror version of the materials production reactor is based on a design using the axicell end-cell configuration, utilizing electron thermal barriers. This plugging scheme was chosen as the most attractive design during Lawrence Livermore National Laboratory's (LLNL's) FY 81 comparative study of different end-plug designs.[3] The same end-cell configuration was also chosen for use in the MFTF-B experiment and the pure fusion reactor Mirror Advanced Reactor Study (MARS). A detail drawing of one of these end cells is shown in Fig. 2; a schematic of the profiles of confining potential ϕ and magnetic field B is shown in Fig. 3. Figure 4 is an isometric view of the end-plug configuration for the baseline TMPR.

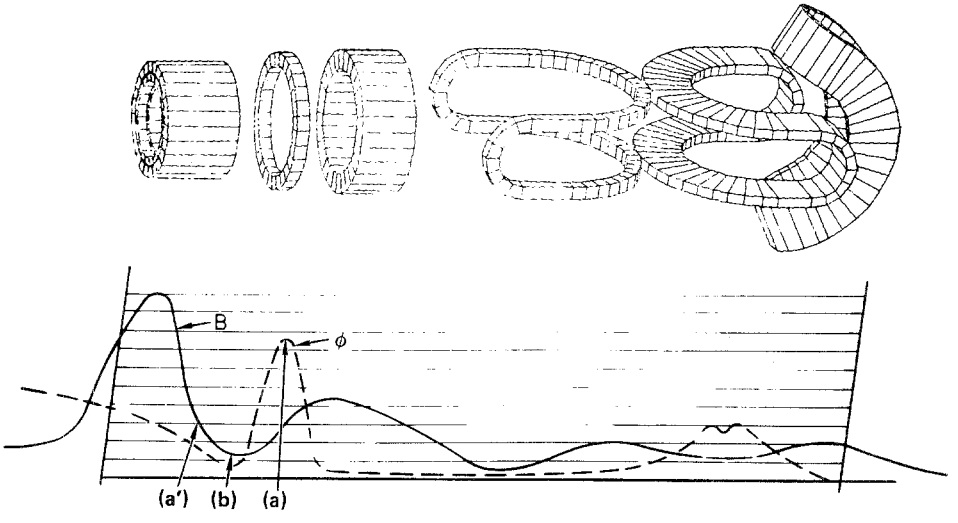

Fig. 3. Axial profiles of confining potential ϕ and magnetic field B for the baseline case.

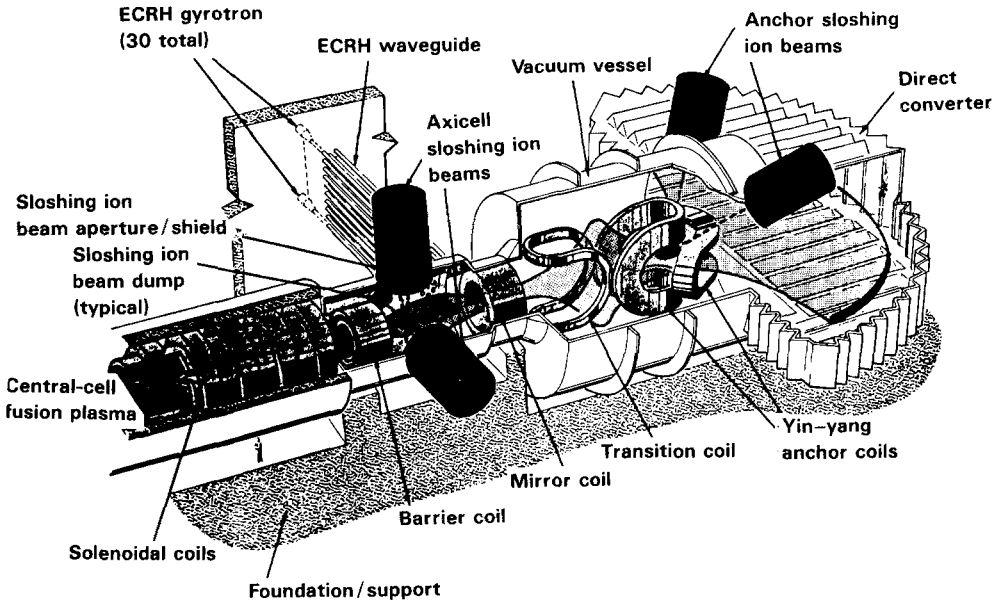

Fig. 4. Tandem mirror reactor axicell configuration.

The name "axicell" was given to this plugging scheme since the majority of ions passing from the central cell to the end-cell region experience only azimuthally uniform magnetic fields, produced by compact, high-field, circular coils. The thermal barrier mode was chosen in favor of the "two-component" or "Kelley" modes[4] because of the superior performance achievable at the small sizes appropriate for this application. Nonaxisymmetric "Yin–Yang" magnets at the ends provide a good curvature region that stabilizes the configuration to gross lateral motions of the plasma column. These motions are thought to be the most unstable, fluidlike modes present in tandems. For this reason, these regions of the machine are called "anchors."

The end regions of the reactor currently require the most advancement and development, both in the physics of operation and the technology needed to build and heat them. The thermal barrier concept is currently being tested on TMX-Upgrade (TMX-U), which has been operated since summer 1982. Plug microstability through the use of "sloshing" ions has been successfully tested on TMX-U. Issues regarding the MHD stability of average minimum $|B|$ configurations, when only a small population of particles sample good curvature, have been raised recently[5] and are currently being evaluated in detail.[6]

Three areas of fusion component technology require development. High-energy, negative-ion neutral beams (~ 450 keV) and gyrotrons, which have single-tube power outputs on the order of 1 MW and in the frequency range of 100 GHz, are needed. In addition, compact, circular, hybrid magnets producing on-axis field strengths of 20 T should be developed. Subsequent sections of this report will describe the development plan required to realize this level of physics understanding and component performance.

The central-cell region around which the breeding blanket is wrapped and the Yin–Yang magnet anchors, which provide good curvature for MHD stability, require virtually state-of-the-art magnet technology, utilizing NbTi superconductors. Only small extrapolations in our current knowledge, recently acquired with the successful operation of the MFTF Yin–Yang, are necessary to make these components work in the materials reactor.

The plasma parameters for the tandem mirror materials reactor are listed in Table I. This reactor has a ratio of fusion power to trapped injected power, denoted as Q, of about 4.5. The ratio of central-cell plasma pressure on axis to magnetic field pressure β_c was taken to be a conservative 40%. A value this high was demonstrated locally in TMX during intense neutral beam injection. The magnetic field strength of the central cell is 4 T on axis, which translates to an on-conductor field strength of about 6 T, well within the range in which NbTi superconductors are applicable. The minimum first-wall radius, computed to be about 0.7 m, combined with the 50-m central-

Table I. Baseline Physics Case for Materials Production Reactor

Parameter	Value	Parameter	Value
Central cell		Axicell/barrier	
Density, n_c (cm^{-3})	2.4×10^{14}	Beta at point *a*, β_a	0.47
Ion Temperature, T_c (keV)	30.0	Barrier potential dip, ϕ_b (keV)	151.0
Electron temperature, T_{ec} (keV)	23.0	Ion-confining potential, ϕ_c (keV)	102.0
Plasma radius, r_{cc} (cm)	47.0	ECRH frequency applied at point b (GHz)	50.0
Vacuum magnetic field, $B_{c,vac}$ (T)	4.0	ECRH frequency applied at point a (GHz)	82.0
Beta, β_c	0.4		
Floating potential, ϕ_e (keV)	173.0	Anchor	
Cold fueling current, I_c (kA)	0.26	Anchor plasma radius, r_{anch} (cm)	0.67
Ion-confinement parameter, $(n\tau)_i$ ($s\cdot cm^{-3}$)	8.1×10^{14}	Anchor effective length, L_{eff} (cm)	2.8
Electron-confinement parameter$(n\tau)_e$ ($s\cdot cm^{-3}$)	7.2×10^{14}	Sloshing beam trapping fraction (%)	0.2
		Sloshing ion energy, $E_{slosh,anch}$ (keV)	150.0
First-wall radius (cm)	67.0	Hot-ion density, $n_{slosh,anch}$ (cm^{-3})	1.6×10^{13}
Central-cell length (m)	50.0	Anchor ion-confinement parameter, $(n\tau)_{i,anch}$ ($s\cdot cm^{-3}$)	5.4×10^{12}
		Anchor floating potential, ϕ_{anch} (keV)	111.0
Axicell/barrier			
Maximum hybrid coil field, B_{max} (T)	20.0	Plasma power balance	
Sloshing ion injection energy, $E_{inj,a}$ (keV)	150.0	Axicell beam power (MW)	13.4
Vacuum magnetic field at barrier minimum, point *b* (T)	2.3	Anchor sloshing beam power (MW)	4.0
		Axicell charge-exchange pumping power (MW)	53.3
Total barrier beta ($\beta_\perp+\beta_\parallel$)	1.2	ECRH power applied to barrier minimum, point *b* (MW)	13.1
Perpendicular barrier beta, $\beta_\perp$	0.7		
Passing ion density at point *b*, $n_{pass,b}$ (cm^{-3})	5×10^{12}	ECRH power applied to potential peak, point *a* (MW)	5.5
Hot-electron energy at point *b*, E_{eh} (keV)	500.0	Fusion power (MW)	400.0
Warm-electron energy at point *a*, T_{ew} (keV)	60.0	End-cell fusion power (MW)	27.0
Barrier length, L_B (m)	7.0	Neutron wall loading (MW/m^2)	1.5
Cold-electron density fraction, F_{ec} (%)	0.01	Plasma Q (P_{fus}/P_{inj})	4.5
Sloshing beam trapping fraction (%)	0.3	$\eta^a Q$	1.3
Pump-beam trapping fraction (%)	0.87		

[a] n is the efficiency of plasma heating by neutral beams and microwaves, including trapping fractions and heating-power-generation efficiencies. The power-generation efficiency is taken to be 50% in all cases.

cell length and 400-MW fusion power, results in a neutron first-wall loading of 1.5 MW/m^2, which is adequate for the intended purpose. (An additional 40 MW of fusion power is produced in the end cells.) To fuel the central-cell plasma, an external source of particles comprising about 260 A is necessary. This fueling will supposedly be accomplished using frozen D–T pellets; related calculations of pellet penetration and fueling are being carried out in support of the MARS. The on-axis field strength of the high-field barrier coil is 20 T. The coil assumed to produce this field strength is a "hybrid coil" with outer layers of NbTi and Nb_3Sn superconductors and an inner, normal-conducting insert coil that is exposed to fields larger than 12 T. This insert coil will consume electrical power, which must be included in the overall power balance. A cross-sectional view of a representative "hybrid coil" is shown in Fig. 5. In the axicell/thermal barrier region, a sloshing ion neutral beam of 150 keV energy must be injected at point "a" in Fig. 3. This beam could conceivably be made from positive ions, which have a broader existing experimental base than beams made of negative ions. This beam must deliver 45 MW of power to the plasma surface; 30% of this beam is deposited in the plasma. The electron thermal barrier region in the axicell must be pumped by neutral beams to keep the barrier potential low. A total of 61 MW of pumping power is necessary to maintain the barrier potential dip, at point "b" at 150 keV (Fig. 3). The three beams necessary to do this pumping are called the low-, medium-, and high-energy pump beams (LEPB, MEPB, and HEPB). The low-energy pump beam has an energy of about 20 keV, has to deliver 0.56 MW of power, and can be produced by positive ions. The medium-energy pump beam has an energy of 66 keV and must deliver the majority of the power, about 44 MW. This beam may also be produced by positive ions. If positive ions are used, it is advantageous if a large fraction of the ions (~ 97%)

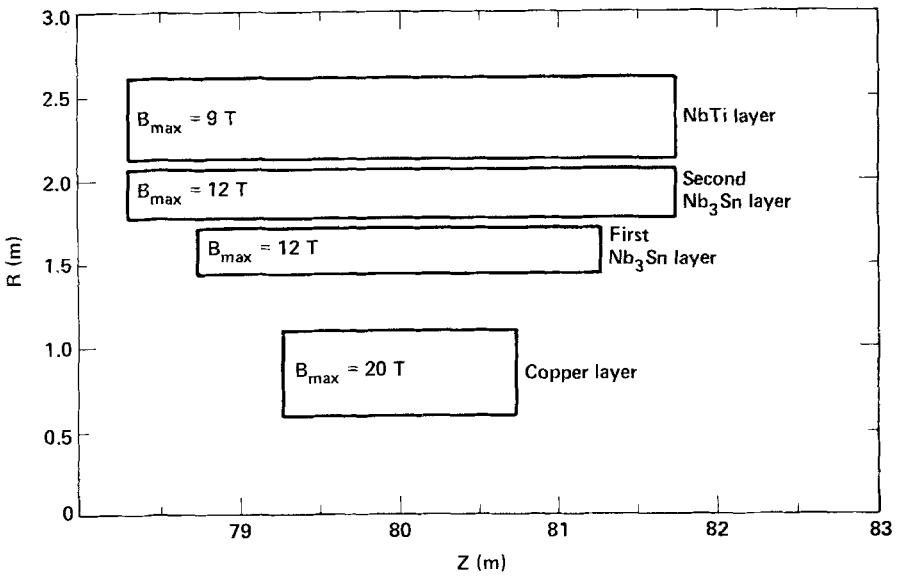

Fig. 5. Cross-sectional view of the 20-T hybrid coil.

accelerated in the beamline is monoatomic. Both the low- and medium-energy pump beams have about a 90% trapping efficiency in the plasma. The high-energy pump beam has an energy of 150 keV but must supply only about 5% of the pumping current, amounting to 16.8 MW of incident beam power, trapped in the plasma at an efficiency of 80%. In the Yin–Yang anchor, it is necessary to inject 20 MW of 150-keV neutral beams produced by positive ions. These beams are injected at an angle with respect to the magnetic field at the midplane, thereby producing a double-peaked "sloshing" distribution. They will be deposited in the plasma with an efficiency of 20%.

Electron cyclotron resonant heating (ECRH) is directed at two places in the end cell. The electron thermal barrier requires that hot, mirror-trapped electrons be produced by ECRH at point "b" (Fig. 3). If fundamental heating is used, these electrons will require 14.5 MW of power at a frequency of about 60 GHz. An ECRH will also be required at the potential peak (point "a" in Fig. 3). Estimates suggest that about 6 MW of power are needed at 90 GHz. A trapping efficiency of 90% is assumed for both ECRH powers.

A power-flow diagram of the tandem mirror plasma driver is shown in Fig. 6. In addition to the end-cell beam and ECRH powers mentioned above, one should note the 8 MW of charged particle power that is deposited into the cold tenuous surface or "halo" plasma. This radial particle flow is a consequence of the α ash-removal scheme that causes radial transport of both alphas and D–T ions. This heat source to the halo ensures that its density and temperature are high enough to provide a good shield for the hot plasma.

2.1.2. *TMPR Case-Stable to Trapped-Particle Modes*

A new mode to which tandem mirrors are susceptible has recently been discovered[5] and can exist unless certain precautions are taken. Avoidance of the so-called "trapped-particle mode" requires that a minimum fraction of the central-cell ions pass into Yin–Yang anchors where the stabilizing good curvature is. In the design depicted in Figs. 2 through 4, insufficient ions are allowed to sample the fields in the Yin–Yang and it is, therefore, unstable to this mode. One way to suppress the mode is to move the thermal barrier (point b) and the ion-confining potential peak (point a) to the Yin–Yang anchor. In this configuration only neutral beams are injected into the axicell (i.e., no ECRH) to produce a bump in potential on the order of the central-cell ion temperature. This bump controls the amount of density that passes through the Yin–Yang to satisfy the new trapped-particle mode criteria to any desired safety factor. There is a tradeoff between enough density to stabilize the mode and too much density, which will degrade Q.

The region between the axicell and the Yin–Yang is called the transition region; it must be pumped

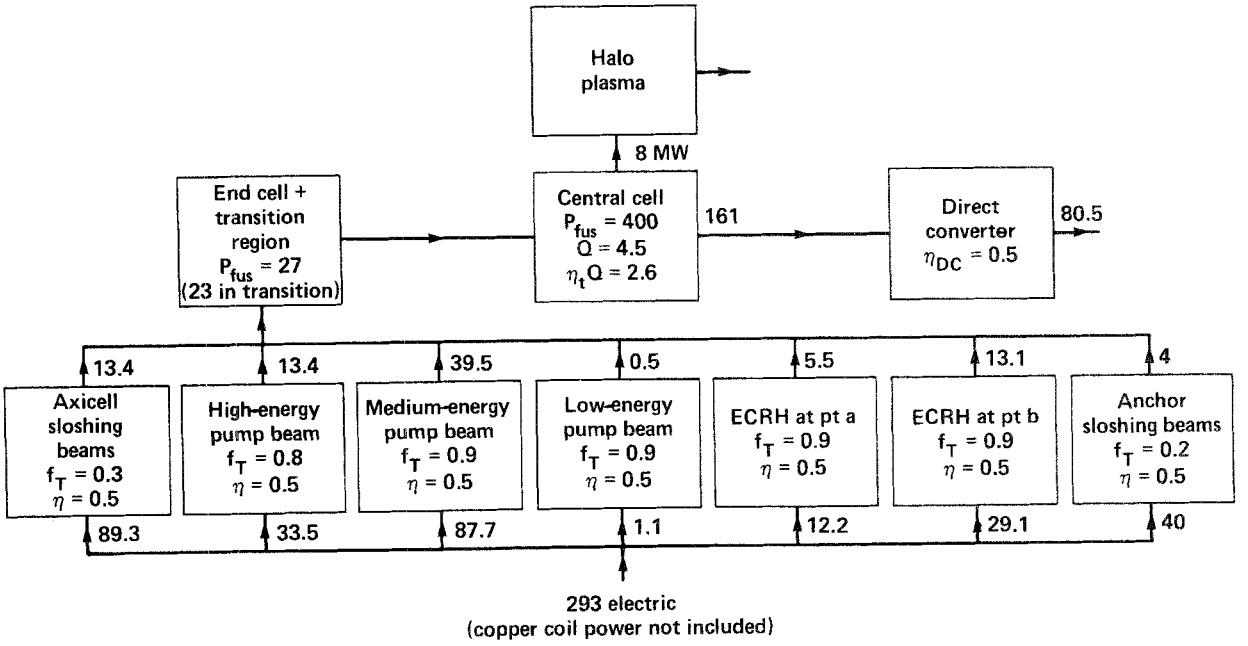

Fig. 6. Plasma power flow for the tandem mirror production reactor.

(with an MEPB) in the new configuration. This charge-exchange pumping is required because the density in the region is higher than in the axicell design in Fig. 3. Too much density (e.g., pressure) in the transition region will make it difficult to design a magnet coil set that will confine a high-pressure plasma effectively. Current work in support of MFTF-B, the Technology Demonstration Facility (TDF), and MARS is aimed at finding a transition-region magnet design that will exhibit the desired MHD stability properties.

Table II shows the physics parameters for a representative new case that is stable to trapped-particle modes. The gross performance of the machine is similar to the baseline case described earlier and to parameters listed in Table I. Notable differences include a 2-T increase (from 4 to 6 T) in the central-cell magnetic field and a corresponding decrease in the plasma radius to obtain the same fusion power for fixed central-cell length and β. This was necessary to satisfy trapped-particle-mode stability criteria that favor small radii and high central-cell fields. Also, the higher fusion-power density results in a wall loading of about 2 MW/m^2. In addition, the model has been improved to include a finite α particle concentration ($\sim$10%) achieved by radial transport caused by nonaxisymmetric magnetic fields. These fields also cause radial transport of D–T fuel and are reflected in the value of the $(n\tau)_i$ for D–T. The axicell magnetic-field configuration has been altered considerably; most noticeably, the peak axicell field occurs at the outboard, rather than the inboard, mirror, and fields at the lower mirror and midplane are considerably higher than in the old configuration. In fact, copper/s.c. hybrid coils will be needed for both axicell mirrors, whereas the old design needed them only for the inboard mirror. These high fields are used to produce a hot, mirror-confined plasma at reasonable β so that an adequate throttling potential bump $\Delta\phi_{pc}$ can be built. A single charge-exchange pump beam is injected in the transition region at the point where the magnetic field is 10 T; it requires only a moderate energy of 45 keV. This beam can, except for about 10% of the required pumping of deeply trapped particles in the thermal barrier, pump trapped particles in both the transition and barrier regions. This residual pumping is accomplished with the recently invented AC∇B pumping coils.[7]

The requirements for the neutral beam injector have changed appreciably from those of the baseline. The axicell requires a tritium neutral beam that has an energy of 200 keV. The sloshing neutral beam in the barrier region requires an energy of 475 keV, compared to 150 keV in the baseline case. It is thought that this energy can, at the expense of sloshing beam power and current, be reduced to around

Table II. Physics Case-Stable to Trapped-Particle Modes

Parameter	Value
Central Cell	
Fraction of thermalized α particles, $C_\alpha = n_\alpha / n_c$	0.1
D–T ion density, n_c (cm^{-3})	2.87×10^{14}
Ion temperature, T_i (keV)	30.0
Electron temperature, T_{ec} (keV)	29.6
Plasma radius, r_{cc} (cm)	38.0
Vacuum magnetic field, $B_{c,vac}$ (T)	5.0
Beta, β_c	0.4
Floating potential, ϕ_c (keV)	199.0
Cold fueling current, I_c (kA)	0.21
Ion-confinement parameter $(n\tau)_i$ ($s \cdot cm^{-3}$)	3.25×10^{14}
Electron-confinement parameter $(n\tau)_e$ ($s \cdot cm^{-3}$)	4.14×10^{14}
First-wall radius (cm)	54.0
Central-cell length (m)	50.0
Axicell	
Injection energy (keV)	200.0
Injected species	Trititium
Total density (cm^{-3})	5.62×10^{14}
Hot-ion density (cm^{-3})	3.74×10^{14}
Hot-ion energy (keV)	334.0
Plasma radius, r_x (cm)	25.0
Axicell length, L_x (m)	2.0
Axicell beta, β_x	0.4
Hot-ion confinement $(n\tau)_H$ (cm^3/s)	6.93×10^{13}
Potential bump height, $\Delta\phi_{pc}$ (keV)	14.5
Inner mirror, B_{x1} (T)	17.5
Midplane vacuum field, B_{x2} (T)	11.7
Outer mirror, B_{x3} (T)	20.0
Transition region	
Length, L_t (m)	5.83
Vacuum field at midplane, $B_{vac,t}$ (T)	1.6
β_t	0.124
MEPB injection energy, E_{pump} (keV)	45.0
Pump-beam injection angle, Θ_{MEPB} (degrees)	25.0
Passing D–T density at midplane, $n_{pass,t}$ (cm^{-3})	4.645×10^{12}
Plug/barrier/anchor	
Vacuum field at barrier midplane, $B_{vac,b}$ (T)	2.2
β_b	0.5
Passing D–T density at midplane, $n_{pass,b}$ (cm^{-3})	3.97×10^{12}
Hot-electron energy, E_{eh} (keV)	280.0
Warm-electron temperature, T_{ew} (keV)	103.0
Cold-electron density fraction, F_{ec}	0.033
Mirror-to-mirror length, L_b (m)	6.0
Inner Yin–Yang mirror, B_{Ai} (T)	7.0
Outer Yin–Yang mirror, B_{Ao} (T)	6.0
Sloshing ion injection energy, $E_{inj,A}$ (keV)	475.0
ECRH frequency at point "b" (hot electrons) (GHz)	43.0
ECRH frequency at point "a" (warm electrons) (GHz)	73.0
Barrier potential dip, ϕ_b (keV)	175.0
Ion-confining potential, ϕ_c (keV)	100.0

Table II. *Continued.*

Parameter	Value		
Plasma power balance	Trapped	Value	Incident
Axicell neutral beam power, $P_{nb,x}$ (MW)	8.54		8.83
Anchor sloshing beam power, P_{slosh} (MW)	4.6		12.3
ECRH power to hot electrons, $P_{ech,b}$ (MW)	55.3		61.4
ECRH frequency applied to hot electrons, $w_{ech,a}$ (GHz)		40–60	
ECRH power to warm electrons, $P_{ech,a}$ (MW)	2.8		3.1
ECRH frequency applied to warm electrons, $w_{ech,a}$ (GHz)		70–90	
Pumping power in transition and barrier, P_{pump} (MW)	29.3		29.3
Fusion power, P_{fus} (MW)		400.0	
End-cell fusion power (MW)		40.0	
Neutron wall loading (MW/m^2)		1.9	
Plasma Q (P_{fus}/P_{inj})	4.0		3.5
η^{I}aQ		1.75	

[a] η is the efficiency of plasma heating by neutral beams and microwaves, including trapping fractions and heating-power-generation efficiencies. The power-generation efficiency is taken to be 50% in all cases.

300 keV (but not much lower) while still requiring the use of negative ions for this beam. The increase in injection energy was a consequence of moving the sloshing beam injection location from the potential peak (point a) to the inboard turning point of the sloshing ions (point a′). This was made necessary because of physics reasons unrelated to the trapped-particle stability question. If the baseline case in Table II had sloshing beam injection at point a′, an energy of about 300 keV (instead of 150 keV) would be necessary. The ECRH frequencies required are in the 60- to 100-GHz range, not unlike the baseline.

With regard to the injected power required, the largest change between the two cases has been the power required to sustain the hot electrons at point b. The increase from 13 to 55 MW is due primarily to a more up-to-date formula for ECRH-heated hot-electron confinement ($n\tau$) and to effective hot-electron residence volume based on recent Fokker–Planck calculations and is unrelated to stability questions.

The introduction of the additional trapped-particle stability criterion appears to have no effect on the feasibility of the materials production reactor. The use of negative ions for the sloshing ions seems necessary, because of changes in their injection point, for either the old or new configurations. Although more recently obtained scaling laws for ECRH and neutral beam powers change the demand on each subsystem, the total power remains the same but produces a higher wall loading.

2.2. Fusion Component Description

2.2.1. Introduction

Either ECRH or a high-energy neutral beam is required in the axicell region, a number of charge-exchange pump beams (the number depends on whether the case in Tables I or II is considered) are used in the transition region, and two ECRH systems and a very high-energy neutral beam are needed in the barrier region. Table III contains two sets of heating system requirements. Set 1 corresponds to the original axicell configuration with three pump beams (low-, medium-, and high-energy), and anchor and axicell sloshing beams, described in Section 2.1.1. The second set is scaled from a MARS configuration, stable- to trapped-particle modes, with one pump beam, an axicell beam, and an anchor sloshing beam, described in Section 2.1.2. Each of the two configurations has two ECRH systems.

A conceptual design of prototypical ECRH, positive-ion neutral beam (PINB), and negative-ion neutral beam (NINB) systems will be presented. The heating systems are based on the requirements for set

1 above. As a postscript, the impact of the second set of requirements on the heating systems is discussed.

2.2.2. *Electron-Cyclotron Resonance Heating Systems*

The power requirements for tandem mirror reactor (TMR) ECRH systems are much greater than those for current and near-term devices. Since the current experimental ECRH systems are not considered optimal for reactors, various options for each of the major ECRH subsystems were considered in a cost/efficiency trade analysis.[8] The baseline design that evolved from the trade analysis incorporates a Graetz bridge-based power supply, 1-MW gyrotrons with a depressed collector, and a quasi-optical transmission system. The mid-to-late-1990s time frame is assumed to provide adequate time to develop and commercialize these extrapolated technologies.

2.2.2.1. ECRH Power Supplies. Use of the Graetz bridge power supply has precedent in power grid application for ac–dc conversion for dc transmission.[9,10] The conceptual power supply for the production reactor is currently envisioned to be a one-pole system operating at 150 kV for the megawatt gyrotron and consists of one converter group and the main auxiliary components shown in Fig. 7.[10]

Table III. Heating-System Requirements

	Set 1	Set 2
ECRH at point "a"		
Power delivered (MW)	5.1	1.1
Frequency (GHz)	37.2–82.0	
ECRH at point "b"		
Power delivered (MW)	13.2	26.2
Frequency (GHz)	21.6–50.0	
LEPB: positive ion		
Power delivered (MW)	0.56	22.0
Energy (keV)	20.0	50.0
MEPB: positive ion		
Power delivered (MW)	43.9	—
Energy (keV)	66.0	—
HEPB: negative ion		
Power delivered (MW)	16.8	—
Energy (keV)	151.0	—
Anchor: negative ion		
Power delivered (MW)	44.7	11.3
Energy (keV)	250.0	475.0
Axicell: negative ion		
Power delivered (MW)	20.0	23.9
Energy (keV)	150.0	200.0

The converter group draws from a 230-kV ac line and includes six thyristor valves connected as a two-way, three-phase circuit, with a seventh valve as a bypass valve connected between the bus and the ground. Typical bridge data of current systems are

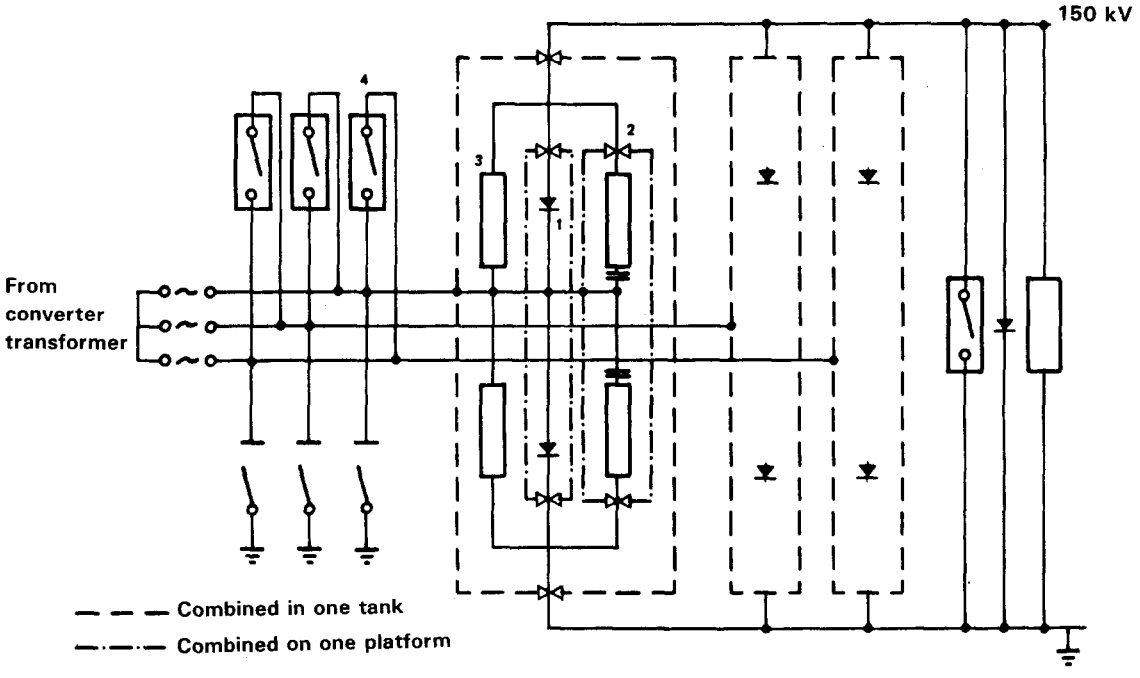

Fig. 7. Simplified bridge-circuit diagram with (1) valves, (2) external dumping circuits, (3) lightning arrestors, and (4) overcurrent divertors.

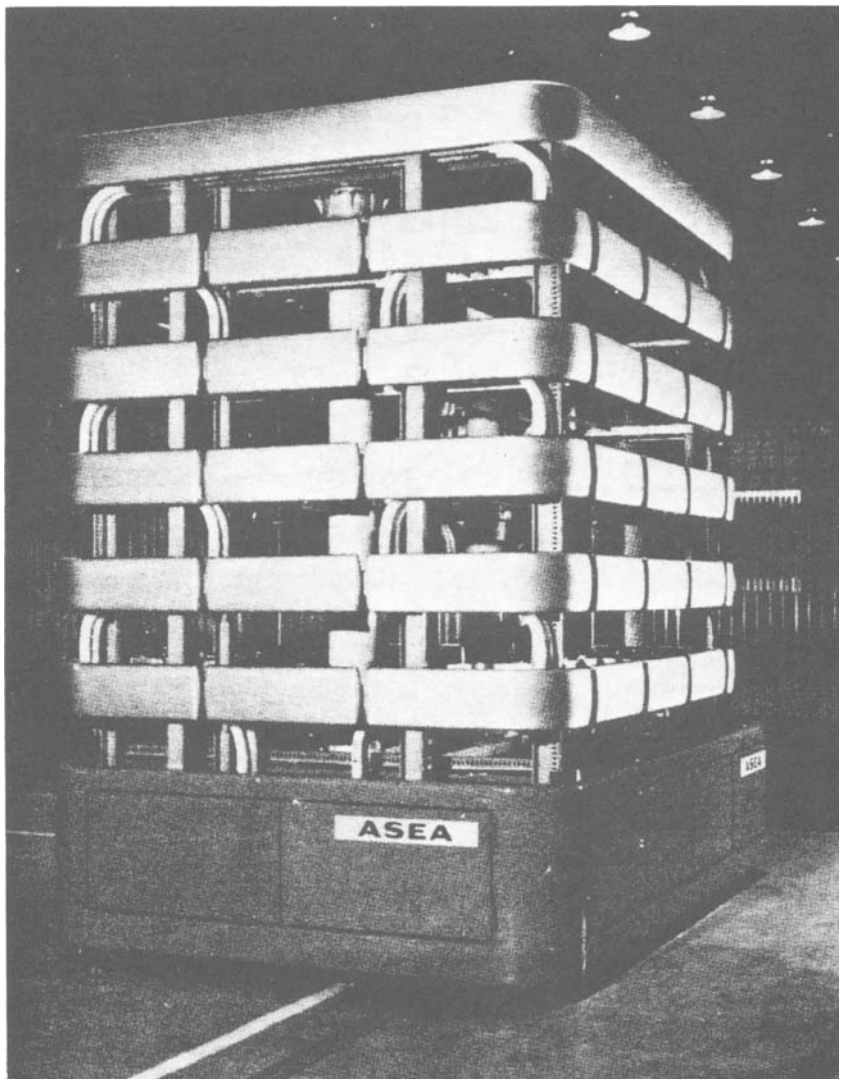

Fig. 8. Water-cooled thyristor valve with a rating of 133 kV and 2160 A, installed at the Sylmar Converter Station of the Pacific intertie.

285 MW, 133 kV, and 2160 A; a valve is shown in Fig. 8.[11] Since this system is larger than necessary for reactor applications, some engineering will be required for scaledown. A thyristor valve can be designed with a minimum number of thyristor devices in series to benefit costs, power losses, and reliability. This power-supply option has several issues and uncertainties in fusion applications that must be addressed in the next level of design. They include the ripple in the dc signal, the fault response time, energy-storage requirements, and the development of a more precise cost estimate.

2.2.2.2. ECRH Sources. Existing ECRH sources are gyrotrons of the microwave cavity type shown in Fig. 9[12] whose powers are limited to < 200 kW in steady state and are only 30–50% efficient. Higher-power sources are desirable for a reactor so that the number of gyrotrons is reasonable and because a cost benefit will occur. The construction of an advanced concept gyrotron is near completion; it should demonstrate higher efficiencies.[13] Several megawatt gyrotron concepts are also being addressed.[14]

Although gyrotrons are the current sources for the ECRH frequency regime, recent concern as to the

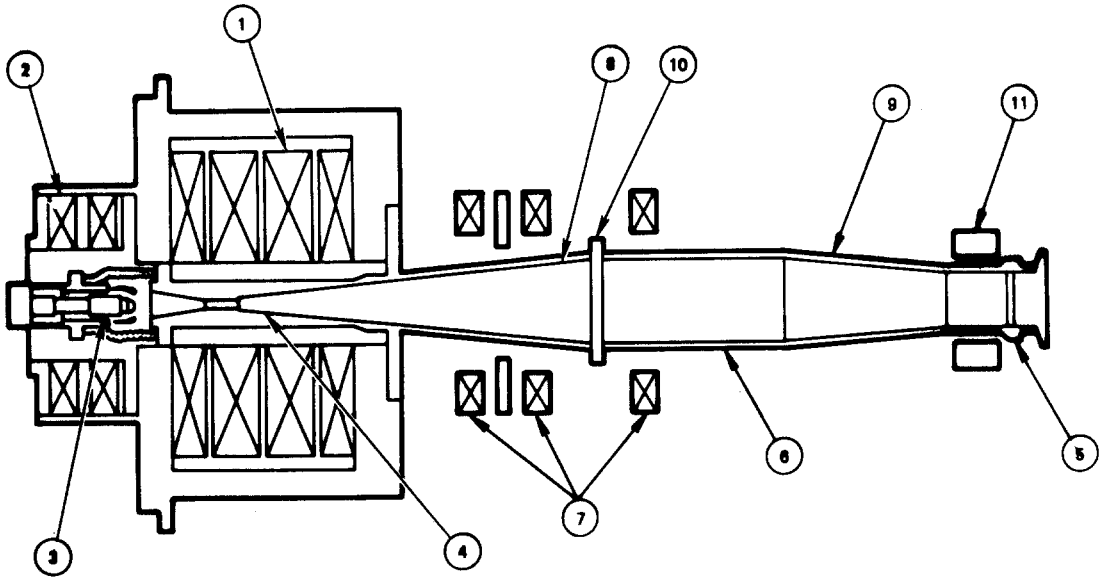

1. Main magnet coils
2. Gun magnet coil
3. Electron gun
4. Cavity
5. Output waveguide and window
6. Beam-collector area
7. Collector magnet coils
8. Output guide up-taper
9. Output guide down-taper
10. Lower collector gap
11. Transverse field magnet

Fig. 9. Conventional gyrotron of a microwave cavity design.

required frequency for efficient heating and penetration during the various stages of startup has caused some interest in free-electron lasers (FELs). These lasers allow for frequency variability and emit a Gaussian wave mode that has some advantages with respect to quasi-optical transmission systems. FELs are not considered in the baseline, however, because a national development plan does not exist.

One disadvantage of the microwave cavity gyrotron in high-power configurations is that the electron beam propagates in the resonant cavity. As gyrotron power increases, the size of the collector cavity must be enlarged to dissipate the beam power, making efficient coupling to the desired mode more difficult. Beam recovery is also considered more difficult in the colinear geometry.

One of the megawatt gyrotron designs, the quasi-optical gyrotron, offers a solution to these problems. The electron beam in this double-cavity device (Fig. 10) traverses the two optical cavities perpendicular to their axis. This concept is the source for the ECRH systems considered here. The gyrotron beam voltage is assumed to be ~150 kV, and the collector voltage is approximately −40 kV. With the depressed collector, the net efficiency of the tube is estimated to be ~80%.

2.2.2.3. ECRH Launcher/Transmission System. The quasi-optical transmission system was selected because of the low-efficiency and window issues associated with an overmoded waveguide transmission system. The basis of a quasi-optical system is the "beam waveguide," where a beam is guided without expansion of energy and without use of metal waveguides or resonators. Antennas or horns emit wave beams whose transverse field amplitudes and phase distributions vary along the path of the beam. These distributions can be duplicated periodically by passing the beam through radially dependent phase transformers. Any diffraction loss is due to the finite dimensions of the transformers.[15]

The launcher for the low-loss beam mode is the dual-mode conical horn with paraboloid reflector.[16,17] A schematic and geometry of the launcher are shown in Fig. 11. Since the horn performs well with a proper mixture of TE_{11} and TM_{11} modes and the gyrotron generates a TE_{on} mode, a series of mode

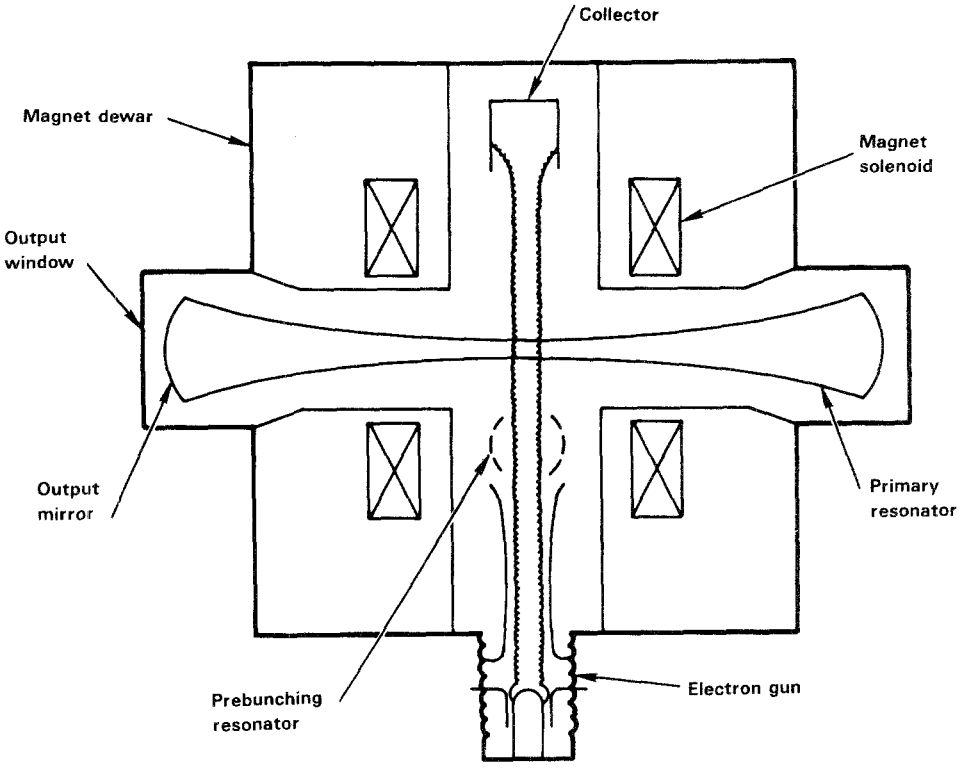

Fig. 10. Quasi-optical gyrotron.

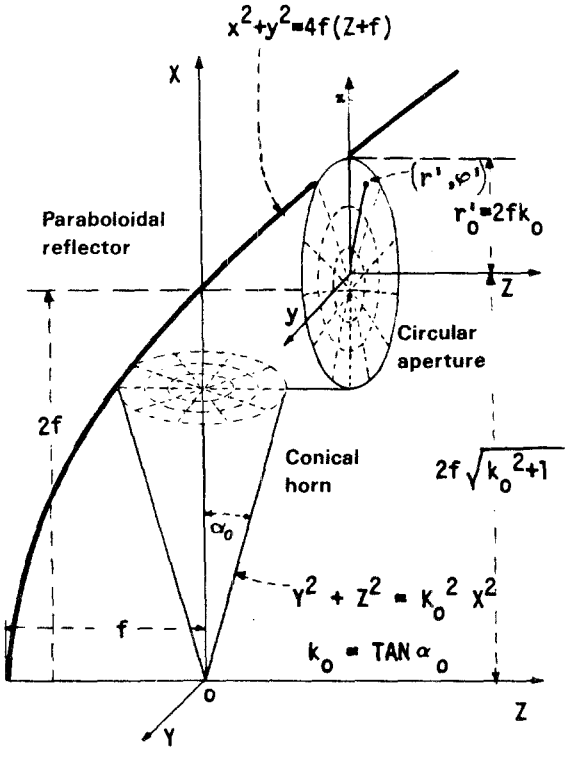

Fig. 11. Geometry of the conical horn-reflector antenna.

converters and/or transducers is required. Conversion occurs in two steps: (1) a $TE_{on} \rightarrow TE_{11}$ converter, and (2) a $TE_{11} + TM_{11}$ converter. Converters of this type have been demonstrated at low power levels (watts) with ~ 5% power loss.[18]

An example of the latter converter is shown in Fig. 12.[19] The launcher provides a linearly polarized plane wave with a Gaussian radial electric field distribution for the lowest loss beam mode.

To hold losses to a minimum, the phase transformers are high-reflectivity mirrors. An offset casegrain configuration, i.e., source-hyperboloidal-mirror-hyperboloidal mirror is used; this allows the gyrotrons to be shielded from the direct-line-of-sight neutrons. The diffraction loss as a function of mirror spacing and radius is found from Fig. 13.[20]

The quasi-optical configuration for a 13.2-MW, 21.6-GHz ECRH system is sketched in Fig. 14. The system characteristics for this and the 5.1-MW, 37.2-GHz system are defined in Table IV. The gyrotrons and transmission systems will be located in a vacuum vessel adjacent to and connected with the reactor vessel. For protection and servicing, vacuum vessels will exist at the vessel interface and at the gyrotron.

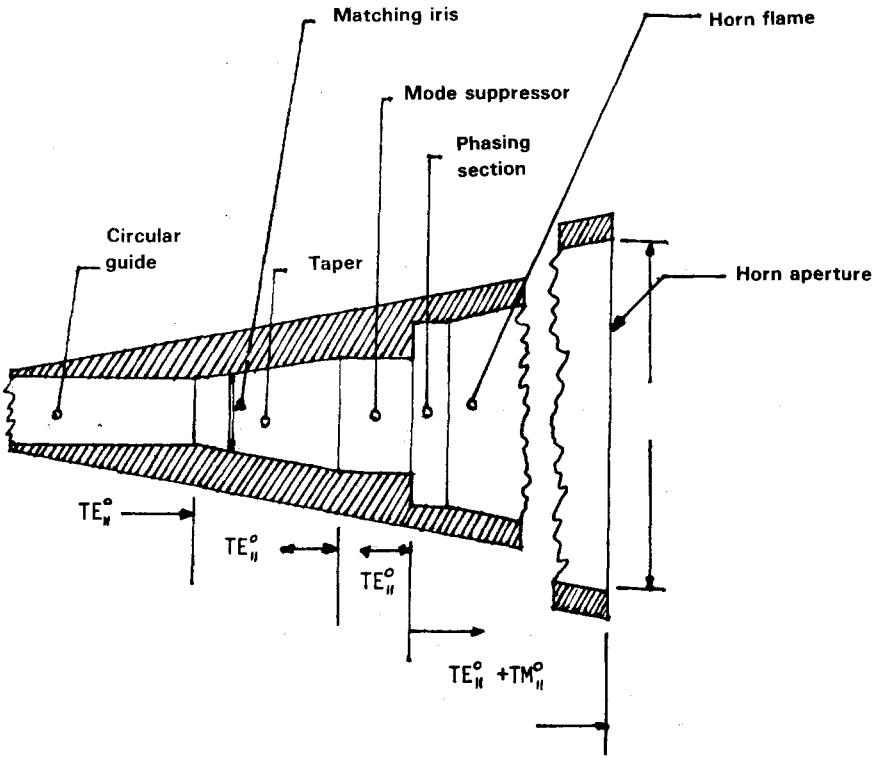

Fig. 12. Dual-mode conical horn conversion.

2.2.3. Positive-Ion Neutral Beam Injector Systems

Positive-ion neutral beam (PINB) injection has proved to be an effective plasma-heating scheme in all magnetic fusion systems.[21-23] But, for tandem mirror reactors, PINBs are also needed to charge-exchange pump the transition region. This application calls for source and beamline constraints over and above those that usually exist in neutral beam (NB) heating systems. Since the early 1970s several key parameters of PINB systems (and the sources in particular) have been continually improved: powers, current density, species mix, and size. Because PINB technology is considerably ahead of that for the ECRH and negative-ion neutral beam systems, fewer technology extrapolations are necessary. The major advance required is long-pulse or steady-state operation.

When the PINB is used to charge-exchange pump, the molecular energy species mix of the beam is critical. If the full energy component is chosen to perform the pumping, partial energy species that are injected and become trapped must also be pumped. The power requirements increase dramatically as the full energy fraction decreases. One option is to place a bending magnet between the accelerator grid and the neutralizer, which removes the molecular species from the beam. This option, however, causes part of the full energy beam to be lost because of neutralization while traversing the magnet region. Table V shows the power characteristics of PINB systems for a number of species mixes and molecular species magnet configurations.

The system requirements for a prototype PINB system, shown in Table III, are delivered full-energy power of 44 MW at a beam energy of 66 keV. The corresponding full-energy current is 667 A. In this study, the design contains rectangular sources with slotted extraction grids. Even though the complexity of the system will increase with the addition of a bending magnet between the extraction grid and neutralizer to remove the molecular species, the gain in recirculating power requirements for the system (because of the noninjection of partial-energy species) dominates the design considerations. The beam passes through the gas neutralizer, through another bending-magnet region in which the unneutralized component of the beam is removed and directly recovered, and through the final duct before the neutralized component is delivered to the plasma.

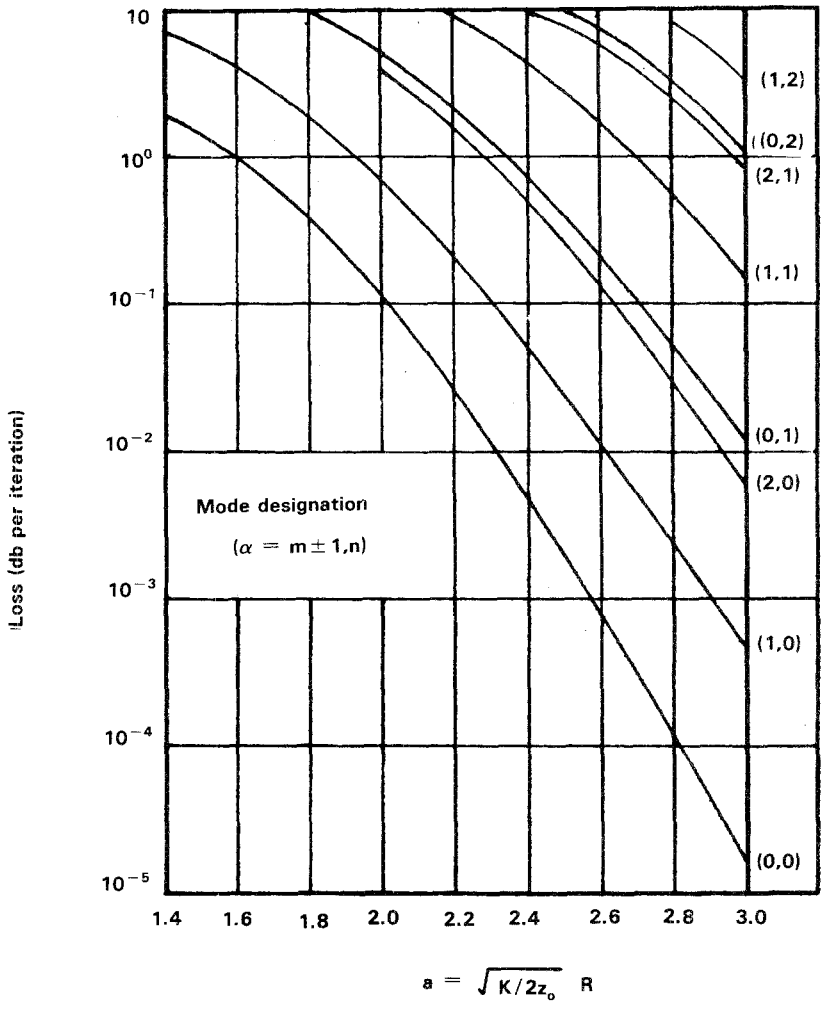

Fig. 13. Iteration loss for various beam modes.

The details on each major system component are discussed in the following sections. Figure 15 is a schematic drawing of the PINB beamline. Twelve operating sources and four redundant sources are arranged with four sources per beamline. Two beamlines charge-exchange pump each end plug.

2.2.3.1. PINB Ion Source / Accelerator. The source is rectangular with a slot-type, four-grid accelerator. The extracted current densities of Tokamak Fusion Test Reactor (TFTR)-type sources are 150 to 160 mA/cm^2, with a grid area of 400 cm^2 (10 cm × 40 cm). The high-full-energy species yield source consists of a field-free plasma source coupled to a 23-cm-deep magnetic-bucket expansion chamber. The filaments are operated in the thermally limited emission mode, enabling longer lifetimes because of lower filament temperatures.[24]

The current NB plasma sources produce a quiescent plasma that, along with plasma density and uniformity, determines plasma quality. The optics of the beam depend on this quality and on the characteristics of the accelerator. With the TFTR sources, divergences (perpendicular and parallel to the slots) of the order of $<1°$ and $<0.5°$, respectively, have been achieved.[24] Since the beamline is 8–12 m long the optical quality of the beam is important. The design of the added bending magnets could have a great impact on the divergence of the system. Specially shaped magnets in the shadow of the extraction grids are currently being considered. These magnets should cause no degradation of the divergence.

Additional source characteristics include a species mix of 85/10/5, a source efficiency of 1 kW/A, and a gas efficiency of 50%. With the re-

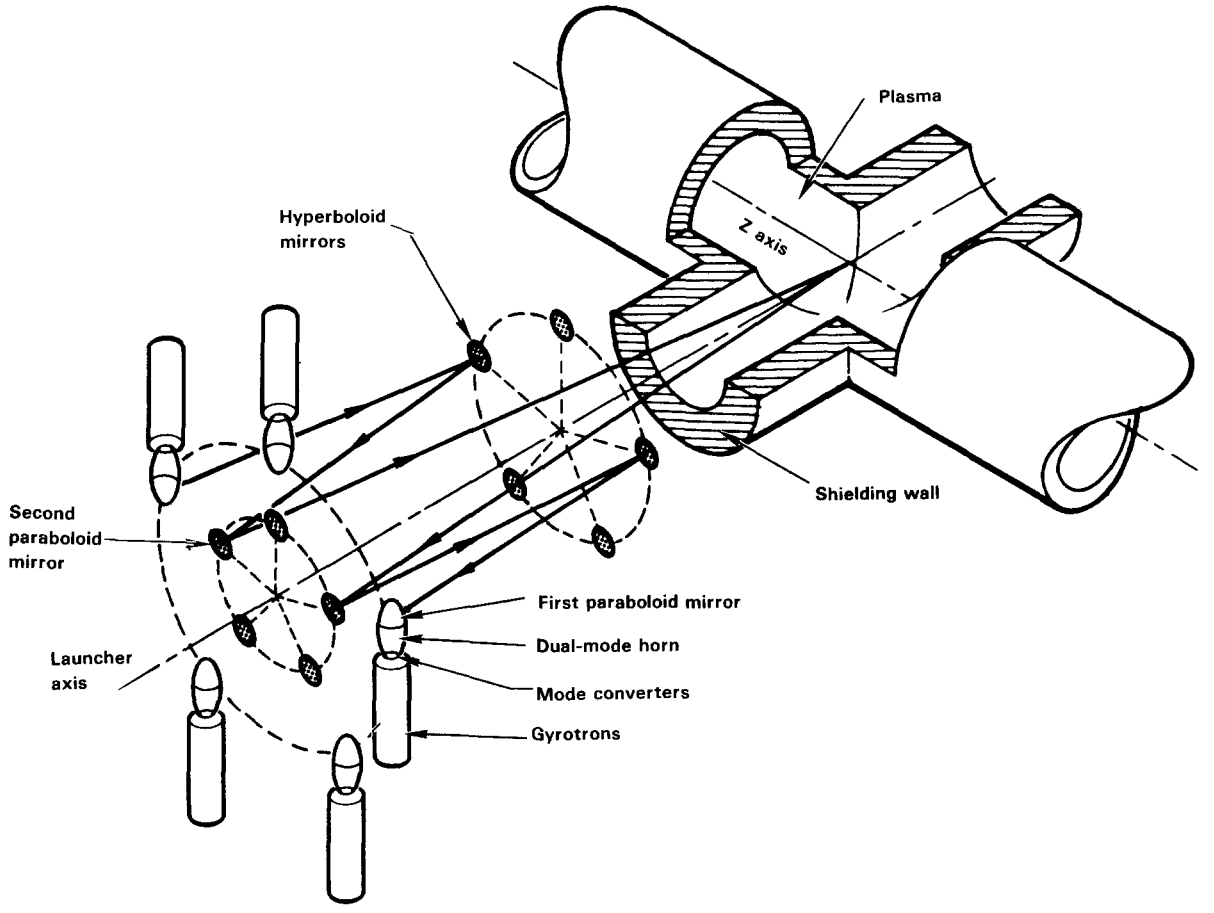

Fig. 14. Quasi-optical configuration of transmission system.

Table IV. ECRH Quasi-Optical Transmission-System Characteristics

Frequency (GHz)	21.6–50.0	37.2–82.0
Delivered power (MW)	13.2	5.1
Ports	4.0	—
Design power per port	3.3	2.6
Gyrotron ports (operating/redundant)	4/1	3/1
Gyrotron power (MW)	1.0	1.0
Angular spread at plasma (degrees)	3	
Diffraction loss per iteration (dB/%)	0.005/1.1	
Reflection loss per iteration (%)	0.4	
Mode-conversion losses (%)	10.0	
Horn loss (%)	5.0	
Launcher focal length (cm)	35.8	27.8
Horn height (cm)	65.7	49.6
Flare angle (degrees)	34.0	
Launcher beam width (cm)	45.0	34.0
Diameter of first mirror on ring (m)	2.1	2.1
Distance from first to second mirror (m)	5.0	
Diameter of hyperboloidal mirror (cm)	45.0	34.0
Diameter of hyperboloidal mirror ring (m)	1.57	
Distance from second poloidal mirror to plasma (m)	10.0	
Diameter of mirror (cm)	63.0	48.0
Diameter of mirror ring (m)	1.05	1.05
Launcher diameter at outer edge of magnet set (m)	1.0	0.85

Table V. Positive-Ion System-Analysis Physics Requirements for Pure Beams Are $P_d = 44$ MW or $I_d = 667$ A at 66 keV

Case	Species mix	p_d^{full} (MW)	I_d^{full} (A)	p_d^{part} (MW)	p_{plug}^{wall} (MW)	System efficiency (%)	Effective efficiency (%)
Partials injected							
	90/7/3	60.8	946	9.7	141.3	50.0	31.1
	85/10/5	84.3	1277	17.3	203.0	50.0	21.6
	80/13/7	138.5	2098	40.5	356.8	50.0	12.3
Molecular species							
Bending mag net (large bend with source and neutralizer decoupled)	85/10/5	44.0	667	—	111.6	39.4	39.4
Magnet (small bend with neutralizer closely coupled to source)	85/10/5	40.0	667	—	110.9	39.7	39.7

mainder of the system defined, currents of 120 A must be extracted from 12 operating sources to deliver 667 A of full-energy particles to the plasma. For 160 mA/cm^2 current density at the extraction grid, a 15-cm × 50-cm source will be adequate.

2.2.3.2. PINB Molecular-Species Bending Magnet. Although a bending magnet between the accelerator and neutralizer eliminates the molecular species and their daughter partial-energy species from the injected beam, its design greatly affects system efficiency and the required grid area. To limit the neutralization and thus losses in this region, the line density must be minimized. If the region to bend the molecular species is long (so they do not enter the neutralizer), the source and neutralizer would have to be decoupled with respect to the gas flow. This decoupling both lengthens the beamline and complicates the pumping system.

Instead, a higher field (~ 4 kG) magnet in the shadow of the extraction grids is 4 cm long in the beam direction and will spread the molecular species along the length of the neutralizer and downstream components. In this case, the source and neutralizer are not decoupled. At an average gas pressure of 3 μ in the magnetic region, 10% of the full-energy component is lost because of neutralization. In this configuration the divergence angles for the separated species are 17.75°, 12.5°, and 10.1° for D_1^+, D_2^+, and D_3^+, respectively. The concept is depicted in Fig. 16.

2.2.3.3. PINB Neutralizer. The neutralizer is a conductance-limiting duct that is oriented to encompass the diverted full-energy beam. The duct is rotated 17.75° from the original beam axis.

The equilibrium neutralizer efficiency at 66 keV is ~17%. Since obtaining this efficiency would require a very long duct (~ 4 m), a design value of 95% of the equilibrium value, or 68%, was chosen. At an average pressure of 1 μ, the neutralizer duct must be 2 m long.

At the diversion angles of the molecular species, the neutralizer duct is long enough to intercept the full-energy species neutralized in the molecular-species bending magnet and in all the molecular species and their products. The power-deposition profile for the particles will have to be determined, and a detailed design will be needed to provide the required cooling, sputtering, etc., of the neutralizer.

2.2.3.4. PINB Beamline. Following the neutralizer, there is a collimator to shape the beam, a bending magnet to remove the unneutralized full-energy components that are then recovered directly, a final collimator, and a drift duct. Together, they deliver a focused full-energy beam to the plasma.

An approximate power flow (shown in Fig. 17a) is attainable without a more detailed design of these components. The beam optics and footprints can be approximated easily. Because of the slit geometry, the beam must be focused in two directions. Consider the X direction in Fig. 17(b) were d is the distance between the extraction grid and the plasma axis and δ is the beam divergence. For the assumed 0.42° and 0.92° divergences and a beamline length of

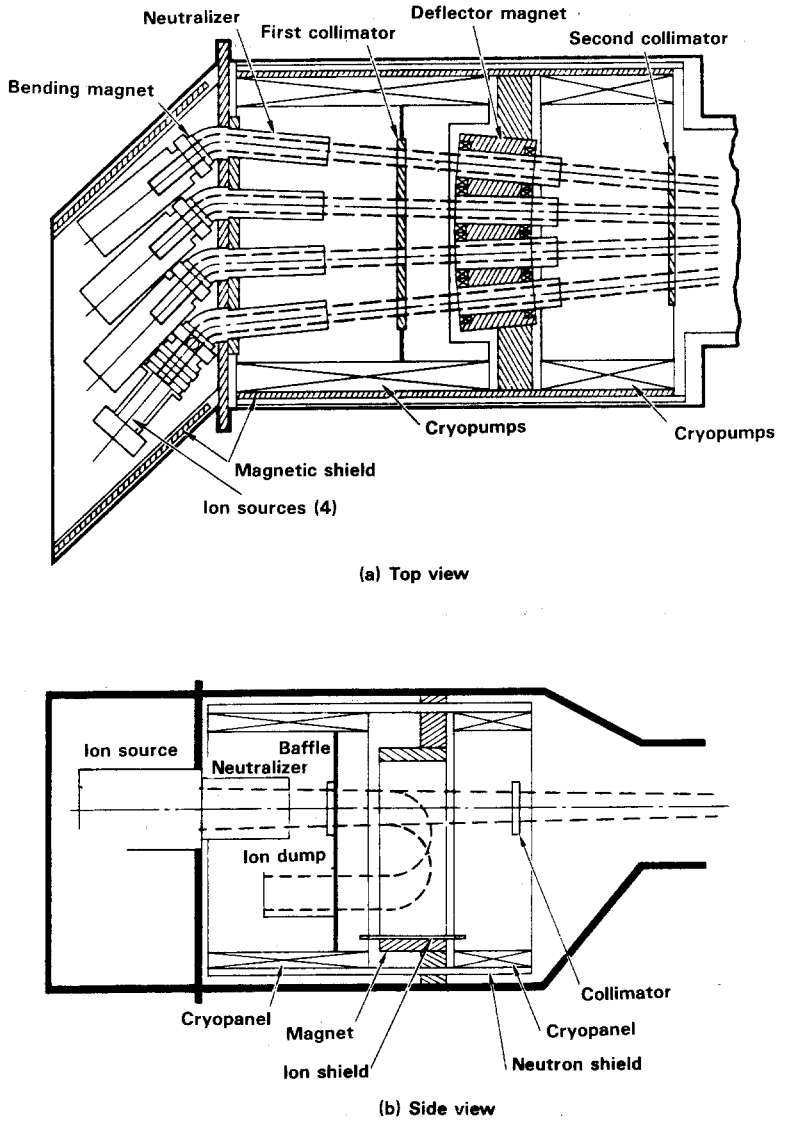

Fig. 15. Schematic drawing of the PINB beamline.

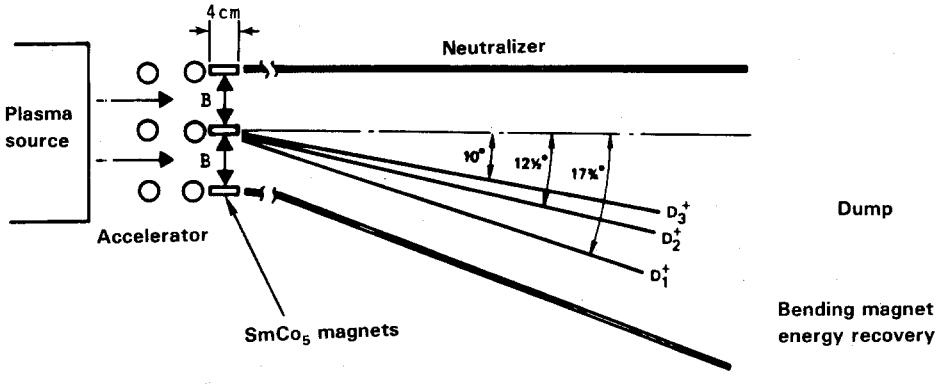

Fig. 16. Geometry of molecular species bending magnet.

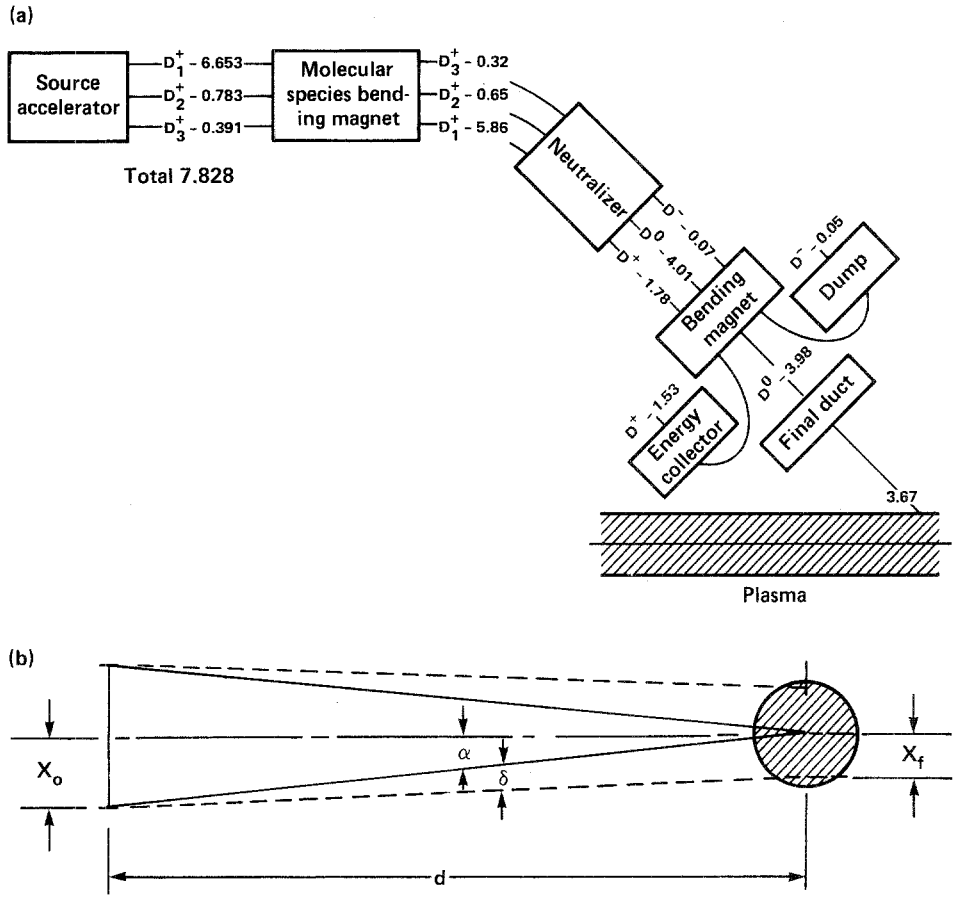

Fig. 17. (a) Geometry of molecular species bending magnet, and (b) geometry for beam-footprint calculation.

11.3 m, the footprint at the plasma axis is 17 cm × 37 cm.

If the magnetic field of the second bending magnet for the unneutralized ions is ~1 kg, the D^+ at all locations in the partially focused beam will be bent 180° to a direct-energy recovery system or dump. The distance between the exit of the bending-magnet region and the plasma axis is ~ 8 m. The drift duct is not necessarily this long; its length depends on the injection angle, the size of the vacuum vessel at the point of injection, and whether the 11.3-m beamline length is assumed to be consistent with magnetic-field shielding requirements and the beam footprint with respect to plasma dimensions. These aspects require further study.

The gas flow per beamline is obtained from the extraction current and the gas efficiency of the source. With four sources per beamline, a gas flow of 10^2 Torr-liters/s requires a volumetric pumping rate of 1.0×10^6 l/s for a gas pressure of 10^{-4} Torr. A maximum cryosystem pumping rate of 10^5 l/s m^{-2} correlates into ~10 m^2 of cryopanels. Since the vacuum vessel for the beamline is quite large, there is more than enough surface area to accomplish the pumping. As a result of the sputtering and outgassing of various surfaces, there is an added contribution to the gas flow, but it is assumed to be negligible compared to the source contribution.

2.2.3.5. PINB System Power Supplies. The neutral beam power-supply system (NBPSS) will provide the power required to operate 12 ion sources. Its configuration is very similar to that of the TFTR NBPSS.[25] The system consists of 12 individual power supplies that are connected so that, when a source goes down, power from the affected supply is diverted to one of the redundant sources.

The NBPSS consists of four major subsystems: an ac/dc conversion system, a modulator/regulator,

the auxiliary system for the arc and filament power, and the instrumentation and control system. The primary system will operate from a utility line (60 Hz, 13.8 kV). The accelerator voltage is 66 kV with a 1% voltage regulation and has an output-current rating of 120 A. The arc and filament supplies are low-voltage (<100 V) and very high-current (thousands of amperes) systems.

2.2.4. *Negative-Ion Neutral Beam Systems*

The medium- and high-energy pump beams, the anchor sloshing ion beams, and the axicell beams (shown in Table III) all provide an incentive to develop negative-ion neutral beam technology. Figure 18 shows the maximum neutralization efficiency of various deuterium species in a D_2 gas as a function of energy. As the beam energy increases above 150 keV, one can readily see that the positive-ion neutralization efficiencies drop below 30%, decreasing steeply to less than 10% for $E_b = 250$ keV. Since the heating systems make up a major fraction of plant recirculating power, it is imperative to develop higher-efficiency systems. Negative ions offer a solution; the approximate neutralization efficiency for gas, plasma, and laser photodetachment neutralizers is 60, 80, and 95%, respectively. However, a proof-of-principle system is needed and several major subsystems of the NINB systems require significant development.

The prototypical NINB system described here is representative of all the systems with 150 keV $\leqslant E_b \leqslant 300$ keV in Table III. Consider a 24-MW system having a beam energy of 200 keV and a delivered current of 120 A.

2.2.4.1. NINB Ion Source / Accelerator. The source configuration is based on a Lawrence Berkeley Laboratory (LBL) self-extraction, negative-ion source.[26] It utilizes a cesiated surface that converts positive ions—formed by an rf plasma generator in a magnetic multipole bucket containment geometry—into negative ions. The cesiated surface is approximately 15 cm from the accelerator, and the electron current from the plasma is suppressed by a transverse magnetic field created by $SmCo_5$ magnets near the extractor aperture. A schematic drawing is shown in Fig. 19.

The current status of this source development is represented by several key parameters: total current = 1 A, slot size = 3 cm × 25 cm, total beam area = 138 cm^2 FWHM, average beam-current density = 7.3 A/cm^2, power efficiency = 10 kW/A, gas efficiency = 13%, and beam pulse length = 7 s. Other source configurations have reported characteristics that are more appropriate for reactor-scale systems (e.g., > 50 mA/cm^2 current density), but they are not as well-characterized as the LBL source. An improved LBL geometry is expected to produce > 2 A of current for the same source area.

In the time frame of this device the source characteristics are more conservative than those cho-

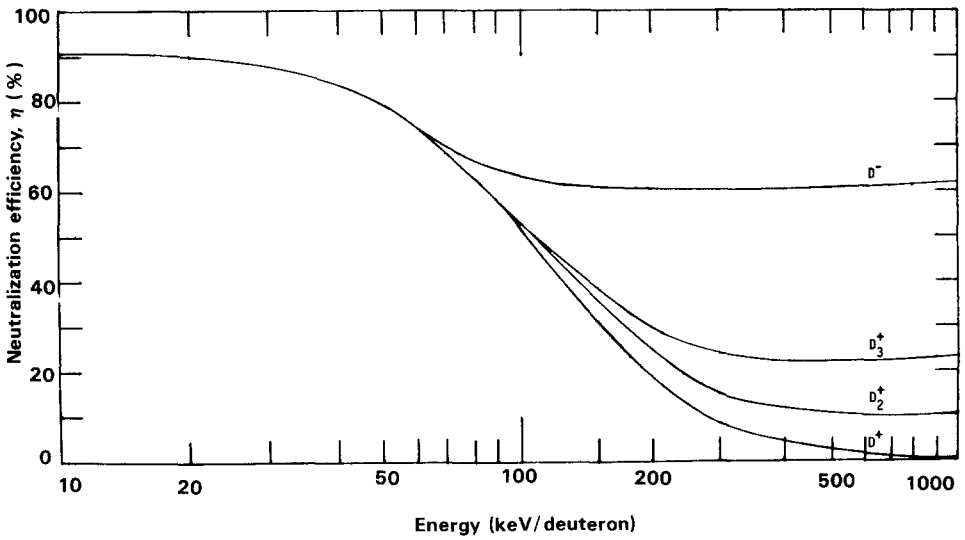

Fig. 18. Maximum neutralization efficiency as a function of beam energy per deuteron.

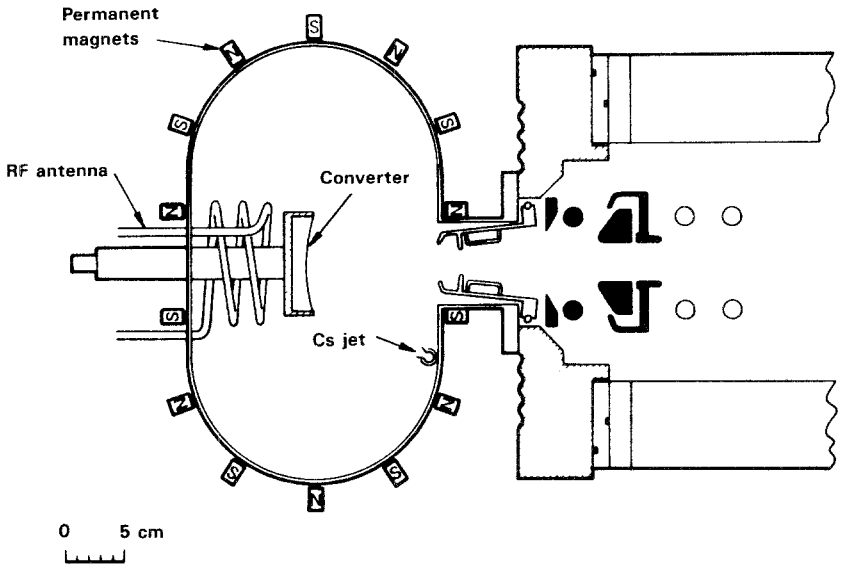

Fig. 19. Schematic drawing of negative-ion source.

sen for MARS, a commercial reactor study.[7] The production reactor sources are assumed to operate at 50 mA/cm^2 current density in a slot whose dimensions are 3 cm × 135 cm. Although the density is an extrapolation of the current LBL source, slot densities of >100 mA/cm^2 have been achieved by the SITEX and hallow-cathode configurations.[27,28] Thus the extrapolation is reasonable.

A single-aperture-dc, multiple-grid accelerator accelerates the source ions to 200 keV. Except for the 475-keV beam in set 2, the accelerator configuration is adequate for the energies of each of the NINB systems considered. The accelerator for the high-energy system is discussed in Section 2.2.5.

Other assumed source/accelerator characteristics are a source gas efficiency of ~30%, a source electrical efficiency of ~5 kW/A of negative current, and an accelerator efficiency of ~85%.

2.2.4.2. NINB Neutralizer. The NINB systems considered here are relatively low-current systems that have a low power requirement. Because of this and the fact that the time frame may not allow for the development of a laser photodetachment neutralizer, only gas and plasma neutralizers were considered.

A plasma neutralizer promises a higher efficiency than does a gas neutralizer because of the absence of shielding of the long-range Coulomb potential in collisions with charged particles and, thus, a larger stripping cross section. Theory[29] and experiments[30] have agreed well with the neutralization efficiency (~80%), but the plasma targets have been rather small. Increased size and integration into a multisource beamline will require much development.

Because the laser photodetachment scheme has the largest potential impact on system efficiency in fusion electric applications, the plasma neutralizer will be developed aggressively only if the laser scheme fails. Hence, the more conservative gas neutralizer has been chosen for the NINB system described here. This neutralizer has a conductance-limiting duct. Since the source pressure is approximately 1 μ, the average duct pressure of 1/2 μ would, for maximum neutralization efficiency, lead to a 2.5-m-long duct. However, additional gas is fed into the neutralizer to increase pressure to the 1-μ value, allowing duct length to be reduced to 1.25 m. The neutralization efficiency is calculated to be 60%.

2.2.4.3. NINB Beamline. Four beamlines, each with three operating and one redundant source, will deliver the 120 A of current to the plasma. Figure 20 shows a beamline schematic drawing. Each source will produce 18.5 A of extracted D^- current, of which 60% is neutralized. The system components that follow the neutralizer are very similar to those of the PINB system described earlier (i.e., collimators, bending magnet, etc.). The unneutralized species, both D^- and D^+, are bent and recovered directly.

Single energy collection allows for a high (80%) collection efficiency. The re-ionization losses of the neutral beam in the deflector magnet region are

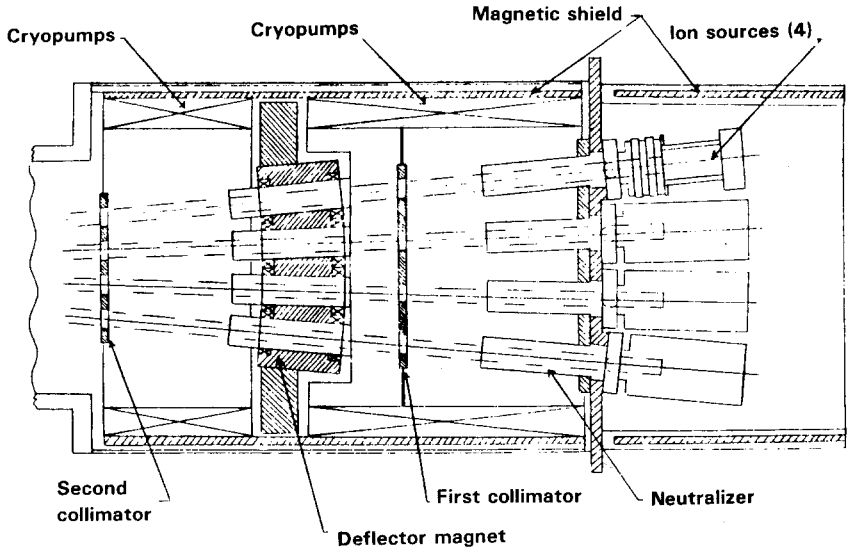

Fig. 20. Negative-ion beamline.

Table VI. System Parameters

Sources	LBL self-extraction
Neutralizer	Gas (60% stripping)
Energy (kV)	200.0
Total current (A)	120.0
Beam area per source (cm)	2.5×160
Current per source (A)	18.5
Sources	12.0
Beamlines	4.0
Source-gas efficiency (%)	30.0
Flow rate per source (Torr-liters/s)	5.5
Source electrical efficiency (kW/A)	5.0
Accelerator efficiency (%)	85.0
Duct transmission (%)	> 90.0
Total gas flow per beamline (Torr-liters/s)	17.7
Total injected power (MW)	24.0
Wall-plug power (MW)	41.3
System electrical efficiency (%)	58.1

calculated to be 2.5%, and the losses in the final duct are estimated at 5%. For the 0.5° × 1° divergence of the source accelerator and a beamline length of 7.5 m, the NINB footprint is 13 cm × 26 cm. The gas flow per beamline of 18 Torr-liters/s requires about 1.8 m^2 of cryopanels, which the vacuum vessel can easily accommodate.

NINB system characteristics are summarized in Table VI. A total system electrical efficiency of 58.1% has been estimated, requiring 41.3 MW of wall-plug power to operate the beamline.

2.2.5. Impact of Variations in Heating-System Requirements on System Design

The past year has seen an evolution of tandem mirror physics and a search for the most attractive tandem mirror reactor. Since heating systems are essential components of the TMR configuration, system requirements have changed as the configuration has evolved. The two cases in Table III are good examples.

The evolution of the TMR has also led to an increased ECRH power requirement. Because frequencies for the respective systems have remained in the same range, the major impact of the changes has been on the number of launchers and gyrotrons and on the increasingly difficult problem of integrating ECRH systems in the complex end-plug geometry. Larger power requirements create an incentive to develop sources with multimegawatt power levels.

The decreased power requirements on neutral beams (in set 2) ease the constraints on system efficiency. The NINB design discussed in Section 2.2.4. included a gas neutralizer rather than a laser photodetachment neutralizer, an undeveloped technology that would be warranted in the higher-power systems of set 1. The lower powers also make integration of the NB systems into the end plugs easier because of the lower number of beamlines (system volumes) and smaller wall area required.

Although the requirements for neutral beam power and negative ion current are more than halved

in set 2, the increased energy requirement of the anchor sloshing beam (to 475 keV) means that an advanced accelerator technique has to be developed. Several accelerator options could be used for the higher energy. Two RF accelerators—the LASL-RFQ and the BNL-MEQALAC—provide high-energy acceleration without high voltages. The electrical efficiencies of these systems are lower than those of dc grid systems because of joule heating and power-supply modulator inefficiencies; the time-averaged current density is also low. The dc electrostatic quadrupole (ESQ) and the dc MEQALAC reduce the probability of breakdown over the entire accelerator column, which is associated with conventional multigrid accelerators. Acceleration in these dc systems occurs between focusing stages over an extended accelerator length; however, none of the four systems is adequately developed and none has been integrated into a beamline.

The most recent reactor configurations[7] call for increased ECRH power, the elimination of the axicell neutral beam that is replaced by an ion cyclotron resonance heating (ICRH) system, and a large pump beam of moderate energy. Although the power levels of this device will differ, the trend will continue.

2.2.6. *Heating-System Costs*

The cost of heating systems can vary dramatically depending on the design used. Heating-system models were developed for a tandem mirror systems code to study the impact of system design on plant capital and operating costs. The models for ECRH, ICRH, and PINB systems were based mainly on previous systems and existing technologies; estimates for the extrapolated technologies are based on the history of similar items. Because negative-ion systems are at an earlier stage of development, costing is somewhat speculative. With the exception of the source, the NINB system discussed in Section 2.2.4. is not fundamentally different than the conventional PINB system.

Table VII displays the costs and several relevant characteristics of the heating systems for the two reactor configurations. The costs are direct costs and do not include estimates for procurement, on-site fabrication and installation, quality and assurance, and profit. The ECRH system cost here differs greatly from current systems and is expected to provide a cost benefit. The low-power system costs are impacted greatly by the redundancy in the systems, evidenced by the cost/watt fluctuation between systems with varying redundancy.

Table VII. Cost Analysis of Heating Systems

	Set 1	Set 2
ECRH at point *a*		
Gyrotron (operating/redundant)	8/2	2/2
Wall-plug power (MW)	8.7	1.9
Efficiency (%)	65.4	64.6
Direct capital cost ($millions)	6.6	2.1
ECRH at point *b*		
Gyrotron (operating/redundant)	16/4	36/4
Wall-plug power (MW)	22.3	44.5
Efficiency (%)	65.4	65.4
Direct capital cost ($millions)	14.1	26.6
LEBP		
Positive-ion sources (operating/redundant)	2/2	6/2
Wall-plug power (MW)	1.2	48.8
Efficiency (%)	48.0	45.0
Direct capital cost ($millions)	1.4	32.3
MEBP		
Positive-ion sources (operating/redundant)	12/4	NA
Wall-plug power (MW)	110.9	NA
Efficiency (%)	39.7	NA
Direct capital cost ($millions)	63.0	NA
HEBP		
Negative-ion sources (operating/redundant)	8/4	NA
Wall-plug power (MW)	29.0	NA
Efficiency (%)	57.9	NA
Direct capital cost ($millions)	30.6	NA
Anchor		
Negative-ion sources (operating/redundant)	12/4	2/2
Wall-plug power (MW)	76.2	18.6
Efficiency (%)	58.6	60.2
Direct capital cost ($millions)	63.7	18.0
Axicell		
Negative-ion sources (operating/redundant)	8/4	12/4
Wall-plug power (MW)	34.6	41.3
Efficiency (%)	57.9	58.1
Direct capital cost ($millions)	34.0	41.9
Total heating systems		
Wall-plug power (MW)	282.9	155.1
Efficiency (%)	51.6	56.3
Direct capital cost ($millions)	213.4	122.1

2.3. Present State-of-the-Art and Development Requirements

2.3.1. Introduction

For plasma physics, the TMPR will require the production of (1) a moderately high β (~ 0.4) central-cell plasma, (2) electron thermal barriers at the ends of the machine, (3) sloshing ions to ensure the microstability of the end plugs, and (4) a viable means for removing thermalized α particles that would otherwise build up to unacceptable levels in the steady state.

For neutral beam component technology, the TMPR[4] will require 10 A of neutral beams at 475 keV, 660 A of a pure beam at 45 keV, and about 40 A of negative ions at 200 keV. With regard to electron heating, the TMPR will require 1-MW gyrotrons producing ECRH at from 40 to 90 GHz. Total power required is on the order of 65 MW. These sources may have to be tunable, with $\Delta\omega/\omega \sim 0.5$, where ω is microwave frequency. For the direct-conversion technology requirement we need a plasma direct convertor (PDC) that can handle about 160 MW of power. This power-handling requirement translates to a direct-converter size requirement that will produce an average heat load of 250 W/cm^2 on the grids. This heat load is thought to be the maximum attainable with liquid- or gas-cooled grids. The TMPR also requires high-field copper/superconductor coils, which will have to be developed.

Tables III and IV compare the physics and technology requirements for the TMPR with those currently shown in experiment for the plasma physics requirements (Table VIII) and with those currently available in the technology (Table IX).

[4]The TMPR case shown in Table II is used for these requirements.

2.3.2. Physics State of the Art and Development

2.3.2.1. Plasma β. One can see from Table VIII that the required high-β, central-cell plasma ($\beta \sim 0.4$)

Table VIII. Comparison of TMPR Physics Requirements and the Current State of the Art (SOA)

Requirement	TMPR	SOA
High-β central-cell operation	0.4 on axis ($\beta = 0.24$) globally in central cell	0.4 locally under neutral beam injection; 0.7 globally, both in TMX
Sufficient energy confinement $(n\tau)_E$	3×10^{14} s/cm^3	3×10^{10} s/cm^3 achieved in TMX; factor of $\sim 10^4$ improvement necessary
Ion temperature, T_i	30 keV	TMX observed 50-eV bulk ions; 250-eV hot ions from neutral beam injection; need from a factor of 100–600 increase
Electron temperature, T_e	30 keV	TMX observed 50-eV electron temperatures need factor of 600 increase
Plasma Q value	4.5	Ion temperature too low to produce appreciable D–T power
MHD stability	Must satisfy criterion for flute and ballooning stability, as well as stability to trapped-particle modes	MHD stability limits have not been pushed in experiment because of heating power availability, and trapped-particle modes have not been observed
Plug microstability	Sloshing ions must suppress microinstabilities	Sloshing ions were recently produced on TMX-U (Summer, 1982) and seem to improve plug microstability
Steady-state operation.-viable α particle and impurity control schemes	Need system to produce $n_\alpha/n_c \sim 0.1$ and keep impurities at low ($\sim 10^{-3}$) level	No α-removal tests now planned. Demonstrated halo plasma shields gas and impurities from hot plasma
Production of thermal barriers	Need full-grade barriers with potential dip, ϕ_b, $\sim$ 5–7 T_e	Thermal barriers have not been demonstrated experimentally. TMX-U will do so in early 1983

Table IX. TMPR Technology Requirements Compared to the Current State of the Art (SOA) and Development Programs

Requirement	TMPR[a]	SOA and DP
Neutral beam systems (a) Positive-ion-based neutral beam system	660 A of pure D^0 at 50 keV, or 1000 A of 90% D^0; 7% D_2^0; 3% D_3^0	80-keV, 80-A beamline developed; 80% D^0, 15% D_2^0, and 5% D_3^0. Efforts to improve species mix is part of DP
(b) Negative-ion-based neutral beam system	40 A at 200 keV; 10 A at 475 keV	1.3-A source in operation at low current density. No beamline developed. Negative-ion-based beamline by mid-1985 per DP
Electron-cyclotron resonant heating	62 MW at 40–60 GHz; 3 MW at 70–90 GHz; tunability may be desired; 1-MW tube necessary	28-GHz (cw), 200-kW tube and 60-GHz, 200-kW tube not tunable. 100-GHz gyrotron at 1 MW in DP for about 1990
Pellet injectors	Pellet velocity from 2 to 10 km/s at 10-pellets/s rate (number of injectors not determined)	Pellet velocity ~1–2 km/s at low repetition rate
Plasma direct-conversion system	250-W/cm^2 average heat load; 160-MW power to be converted	70-W/cm^2 demonstrated plasma source limited. DP has upgrades to approach higher power density
Superconducting magnets	NbTi circular coils; NbTi Yin–Yang	Technology of Yin–Yang and NbTi conductor demonstrated with operation of MFTF Yin–Yang (Feb. 1982). Circular coils are simpler
Copper/superconductor "hybrid" barrier magnet	20 T on axis, 8 T produced by Cu, 12 T produced by superconduction (both NbTi and Nb_3Sn)	Bitter magnets operated at required fields for short periods, but reliability needs improvement. HFTF should prove 12-T conductor technology. A program to develop these coils is needed
Radiation-resistant insulation	High stress resistant at 10^{12} rads	SPINEL is a viable candidate
Tritium-handling systems	See Table XIV	
Remote-maintenance systems	See Volume 2	

[a] Requirements are for physics case of Table II.

has been obtained locally in the central cell by injecting a neutral beam and by trapping a hot, dense, mirror-confined plasma between two of the solenoid coils. Such a demonstration is significant because the economics and plasma performance of the TMPR depend strongly on the value of β attainable.

2.3.2.2. Energy Confinement. In the TMX experiment, the measured energy-confinement parameter for the central cell $(n\tau)_E$ was approximately 10^{10} s/cm^3. The ignited central-cell plasma necessary for the TMPR requires an $n\tau$ value of 3×10^{14} s/cm^3. The four-orders-of-magnitude increase from parameters obtained in the present experiment represents the largest extrapolation of any physics characteristic of the tandem mirror. The large extrapolation reflects the fact that tandem mirror experimentation is, when compared to tokamaks, still in its infancy. However, the MFTF-B experiment, which will go into operation in 1986, is expected to achieve an $n\tau$ value of about 5×10^{13} s/cm^3, only a factor of 10 below the required TMPR performance.

2.3.2.3. Ion Temperature. The central cell of TMX has two ion species: a "hot" component (at ~ 250 eV) produced by neutral beam injection, and a "warm" component (~ 50 eV). The TMPR requires no central-cell injection, but needs an ion temperature T_i of an equivalent "warm" species of about 30 keV. This represents an extrapolation of a factor of 120 from the present hot-species energy and is as much as a factor of 600 above the currently obtained warm-species temperature, which represents a considerable extrapolation. The MFTF-B is expected to achieve ion temperatures on the order of 10 keV, a factor of 3 below that which is required.

2.3.2.4. Electron Temperature. The electron temperature T_e currently achieved in TMX is about 50 eV, while the TMPR operating point dictates a temperature of approximately 30 keV, a factor-of-600 increase from the current experiment. The prediction for MFTF-B is about 9 keV, only a factor of 3 below the requirement.

2.3.2.5. Plasma Q Value. Plasma Q is defined as fusion power production in the central cell divided by the input power required to sustain the end plugs. The TMPR plasma Q is in the neighborhood of 4.5 at a neutron wall loading of about 2 MW/m^2. In the experiment, the central-cell ion temperature (either hot or warm species) is below the threshold for any fusion reactions, even if the central-cell density is comprised of 50% deuterium and 50% tritium. Hence, the Q value obtained for the current tandem mirror is essentially zero. The MFTF-B experiment is expected to achieve an equivalent D–T value of about 0.4.

2.3.2.6. MHD Stability. The TMPR plasma must be stable to gross perturbations that do not bend field lines—the so-called "interchange" modes. It must also be stable to localized perturbations, called "ballooning" modes, that do bend field lines; these modes are expected to become important at high values of plasma pressure. Some evidence from existing tandem mirror experiments (Phaedrus, in particular) indicates that the theoretical interchange criteria are being followed at least at low β. There is not enough heating power in the central cell of present-day tandem mirrors to produce β high enough to test the high-β limits of interchange and the ballooning mode limits. The design of fusion drivers like the TMPR will have to rely on theoretical calculations of plasma stability at this point in time. An experiment like MFTF-B will begin to look at the stability issue experimentally.

2.3.2.7. Microstability. The TMX experiment was plagued with microinstabilities originating in the end cells. Theory has predicted that sloshing ions, which have a specific kind of velocity-space distribution function, will produce the plug microstability desired. The TMX-U experiment, which has recently begun operating, has produced sloshing ions. The end-cell-plasma fluctuation level in TMX-U seems to be less than that in TMX, suggesting that the presence of sloshing ions improves the microstability picture.

2.3.2.8. Electron Thermal Barriers. TMPR performance relies on the production of electron thermal barriers, which have not been produced in any machine. The barriers allow the end-cell electrons to be heated independently of the central-cell electrons, thereby reducing the power to confine ions. The TMX-U is being fitted with the ECRH, which will be necessary to produce barriers, and experiments to produce them should be underway in early 1983.

2.3.2.9. Alpha Ash and Impurity Removal. The steady-state operation of the TMPR relies on the α-particle "ash" and high-Z impurities being removed from the plasma at a rate such that the αs remain at or below 10% of the fuel ion density and the impurities remain low enough for maintenance of a favorable power balance. Reliance only on the axial loss of αs results in an unacceptably high concentration. Schemes that will cause the αs to be radially transported (to obtain the desired loss rate) are now being assessed on paper. This transport is caused by nonaxisymmetric magnetic fields and will affect both αs and fuel ions. Since the high-Z impurities will see a potential hill on the order of 100 keV or more, they will be electrostatically shielded in the central cell. A different means of impurity shielding must be invoked in the end cell because it contains a potential trough (thermal barrier). If neutral gas is to be shielded out throughout the length of the machine, a low-grade "halo" plasma must exist. To date, all of the mirror machines containing hot, dense plasmas that have been studied experimentally at LLNL have had these plasma "blankets." These halos or blankets are effective in shielding the plasma from neutral gas and should be even more effective in shielding out high-Z impurities since the impurities move at much lower speeds than does a neutral deuterium or tritium ion. No α-removal tests are as yet planned. The first D–T-burning machine that could produce α particles naturally would be, perhaps, an upgrade to MFTF-B or the TMNS (Tandem Mirror Next Step).

2.3.3. Technology State of the Art and Development

2.3.3.1. Neutral Beam Systems. Table IX shows, in the area of TMPR technology requirements vs state-of-the-art technology, that the required positive-ion neutral beam technology is, with the exception of the fractional mixture of full-, half-, and third-energy beam components, virtually at hand. If seven of the existing modules are placed at each end of the machine, they will provide the required charge-exchange pumping current. The comparison of what exists and what is required for negative-ion-based neutral beam injectors illustrates the considerable effort needed to arrive at the desired beamline.

Currently, only a 1.3-A source of negative ions exists, producing ions at an unacceptably low current density. What is needed is 40 A of 200-keV negative ions and 10 A of 475-keV negative ions. The sections entitled Sections 2.2.4. and 2.3.4. describe the present development program for negative-ion-based neutral beams.

2.3.3.2. Electron-Cyclotron Resonant Heating. The TMPR requires steady-state powers of ~60 MW of ECRH in the 40- to 60-GHz frequency range to heat the barrier hot electrons and 3 MW in the 70- to 90-GHz range to heat the warm electrons. Based on the economics of producing this power, and the ability to physically locate the gyrotron tubes, a tube with a power output of at least 1 MW is desirable. Because plasma pressure will change the strength of the magnetic field during startup (and the choice of ECRH heating frequency is based on the local magnetic field), tunable microwave sources may be advantageous. Although tuning cannot be accomplished with standard gyrotrons, a source known as the free electron laser is tunable and may have a use in this application. Up to this point, only a modest amount of effort has been applied to the development of FELs. Current state-of-the-art technology for ECRH gyrotrons—28 GHz (cw) in a 200-kW tube and 60 GHz (pulsed) in a 200-kW tube—is now being tested at Varian.

2.3.3.3. Pellet Injectors. Charge-exchange pump beams cannot entirely fuel the central cell; therefore, an additional source of plasma particles is necessary. The central cell plasma is dense enough and the halo plasma shields well enough that fueling by "gas puffing" is not viable. One option, demonstrated experimentally in tokamaks, is the injection of frozen D–T pellets at high velocity. Current injectors are capable of velocities of around 2 km/s. The velocity required for the TMPR depends on the profiles of electron density and temperature that will exist in the machine and on the fraction of the plasma radius the pellet must penetrate. When cubic profiles are assumed for both and 20% penetration is sufficient, a velocity of around 2 km/s is necessary. If flat profiles at 20% penetration are assumed, a velocity of about 10 km/s will be required; this will, of course, necessitate further development. More detailed studies of tandem mirror plasma profiles and fueling will be needed to determine the actual pellet velocity required.

2.3.3.4. Plasma Direct-Conversion System. The direct-conversion system for the TMPR has to convert 160 MW of charged particle power to electricity. Fluid-cooled grids can withstand an average heat load of 25 W/cm^2, which suggests that the required grid area should be 64 m^2. The demonstrated state-of-the-art conversion is a 70-W/cm^2 heat load. This heat load was limited by the plasma source, not by a limitation on power-handling. It was thought that these radiactively cooled grids could withstand a heat load of 100 W/cm^2. The state of the art should be advanced in the area of power-handling capability, testing designs with fluid-cooled grids, in any development program. The efficiency of the direct conversion was on the order of 50% when a module was installed on TMX.

2.3.3.5. Superconducting Magnets. The superconducting magnet technology required for the TMPR central-cell magnets and Yin–Yang "anchor" magnets is in hand with the successful operation of the MFTF NbTi Yin–Yang in early 1982. The size of this magnet is close to that required for the TMPR anchor. The central-cell magnets are larger in radial dimension, but their circular geometry should make them easier to produce than the existing Yin–Yang. The Nb_3Sn technology is needed for the hybrid magnets discussed below.

2.3.3.6. Copper/Superconductor Hybrid Magnet. The TMPR requires a barrier coil that produces 20 T on axis. This will be accomplished with a small-bore circular coil consisting of an inner insert of high-strength copper and layers of Nb_3Sn and NbTi superconductor. The NbTi conductor technology has been demonstrated, and the Nb_3Sn technology is currently being demonstrated in the high-field test facility (HFTF). Copper coils producing the required field strength have been built at the Francis Bitter National Magnet Lab at MIT. These coils have only been operated for minutes at a time, with low reliability, and have smaller bores than required here. A program to develop these normal conducting magnets should be initiated.

For more information, see Sections 4.1.4. and 4.1.5. in this paper and "Remote Maintenance Systems" in Ref. 2.

2.3.4. Existing Development Programs

2.3.4.1. Introduction. Development in several key physics and technology areas is necessary for the TMPR to be introduced in the envisioned time frame (1990s). The physics areas include the production of end-cell plasmas that are free from microinstability, the production of electron thermal barriers, and the demonstration that moderately high-β (~ 0.4)

plasmas can be produced globally in the central cell. Technology development is needed most for neutral beams, continuous cryopumping, microwave heating, and small-bore, high-field, axisymmetric magnets. As discussed below, the plasma physics issues will be resolved on the now-operating TMX-U and on the MFTF-B now under construction. With the exception of the high-field magnets, all of the required technological development is included in the development plan for fusion technologies outlined by DOE in approximately the required time frame. A short discussion of each physics and technology issue follows.

2.3.5. Physics Programs

Previous experiments on the TMX have proved the basic tandem mirror concept: that ions in a long plasma column can be electrostatically confined by a positive potential "hill" produced by intense neutral beam injection in mirror end cells. TMX also demonstrated that plasma β values approaching 40% could be produced in localized regions of neutral beam injection in the central cell. This observation motivated the conservative choice of 40% for central-cell β value in the TMPR. An unresolved problem that plagued TMX was plasma fluctuations in the end cell. These fluctuations enhanced ion heating and transport in the central cell.[5] The introduction of anomalous transport into the reactor scaling model used to generate the TMPR parameters would degrade performance. The fluctuations are thought to be caused by two instabilities—the drift cyclotron loss cone (DCLC) and the Alfven Ion Cyclotron (AIC) instability. These microinstabilities are dependent on the existence of radial density gradients and on the shape of the ion-velocity distribution function. When these modes were identified on TMX and their potential impact on reactor performance was assessed, theoretical work was begun to eliminate them. The current solution is to inject neutral beams perpendicular to the magnetic field, but off the midplane of the Yin–Yang anchor. This results in a velocity-distribution function that is less susceptible to the DCLC and AIC modes.

The axial density distribution is double-peaked, with peaks on either side of the midplane, and is called a "sloshing" distribution function. The production of sloshing ions has been achieved on the recently operating TMX-U (summer, 1982) and is also planned for MFTF-B.

The reactor studies based on the tandem mirror configuration patterned after TMX have shown that very stringent requirements on technology are required to achieve only modest performance. In response to this problem, thermal barriers for electrons were invented. The idea is that, if the axial profile of electric potential in the end plug could have a dip (thermal barrier) right before the potential hill, the cooler electrons from the central cell would be reflected and not penetrate into the region where the potential peak is produced. The electrons that reside in this latter region can then be heated with substantially less power than if the barrier were not there. The dip in potential is produced by a combination of three effects: First, a large mirror magnetic field at the end of the central cell attenuates the ion density in the barrier region, requiring the potential to drop through quasi-neutrality. Second, the way in which the sloshing ions are injected and their density distribution is shaped will aid in the production of the potential dip. Finally, the depth of the thermal barrier can be enhanced by heating electrons to high transverse energy (~ 500 keV) with ECRH so that they become mirror-trapped and axially localized in the barrier region. This excess negative charge will cause a drop in potential to attract an equal number of ions.

The operation of electron thermal barriers with sloshing ions has not yet been demonstrated in the laboratory. TMX-U and MFTF-B will incorporate both sloshing ions and thermal barriers. Very recent results on TMX-U suggest that sloshing ions have been produced successfully and that plug microinstability has improved. TMX-U is just beginning operation, and MFTF-B is scheduled for operation in early 1985. If these demonstrations prove successful, the physics basis necessary for the TMPR will be in hand in sufficient time for its successful implementation.

2.3.6. Existing Technology Development Programs

2.3.6.1. Neutral Beam Injectors. The TMPR will require neutral beam injection at a number of energies and current levels. The more recent physics case in Table II requires injection at 475 keV for the sloshing beam, at 200 keV for the axicell beam, and

[5] Recent results on the TMX-U suggest that some level of plasma fluctuations, while still occurring in the end cells, does not heat the central-cell ions in this larger machine.

at 45 keV for the pump beam in the transition region. On the basis of theoretical considerations of beamline neutralization efficiency, it is preferable to use negative ions at beam energies above about 150 keV and to use positive ions at lower energies. Therefore, both are needed for the TMPR.

The high-voltage test stand (HVTS) at LLNL is currently testing a positive ion source for use with the 80-keV beamline intended for MFTF-B. In 1985 the complete beamline will be operated on MFTF-B. The issue that remains for the 45-keV beam is whether the current of about 660 A can be delivered at the required beam purity (i.e., fraction of beam that is D^0). Current estimates for the MFTF-B species mix is 90% full energy, 7% half energy, and 3% third energy. This species mix would increase the current requirement to about 1000 A. For the pump-beam current to be increased by less than 5%, the fraction of full-energy D^0 would have to exceed 97%; this will require more development work.

The fusion technology development program calls for the completion of a 1-A negative-ion-source demonstration in 1983. Ahead of this schedule, LBL has now demonstrated a 1.3-A negative ion source that operates at low current density. Effort is being spent to increase this current density to more attractive levels. The program plan calls for development of a 10-A negative ion source by mid-1985. The 475-keV anchor sloshing beams for the TMPR require about 5 A of energy per end, making this requirement easily consistent with the development plan. The axicell neutral beams will, more than likely, also require negative ions with energies of 200 keV. These beams require about 20 A of negative ions per end, also consistent with the mid-1985 date for the 10-A negative ion source. The program calls for a 400-keV, 1-MW negative-ion-system prototype, which could be used on the TMPR, to be developed by mid-1995. The negative-ion neutral beam development program is presently receiving only modest support. It is important to develop negative ions for the TMPR.

2.3.6.2. Electron-Cyclotron Resonance Heating. The TMPR requires electron-cyclotron heating at two locations in the thermal barrier/potential peak region. To produce hot electrons, heating of 40–60 GHz is necessary at the bottom of the thermal barrier region. About 60 MW of power at this frequency will be necessary for both end regions. Heating at frequencies between 70 and 90 GHz will be needed to sustain warm electrons at the ion-confining potential peak. There, about 3 MW will be necessary for both ends. The specification of a range of frequencies results from the different requirements during startup and steady state. The higher frequency is necessary during startup when plasma diamagnetism, which reduces magnetic fields and hence resonance frequencies, is below that characteristic of steady state. Also, relativistic effects will reduce the heating frequency not present during startup. To use space efficiently, microwave sources with tube power outputs on the order of 1 MW will be necessary. The currently envisioned microwave source for electron heating is the nontunable gyrotron. The fusion program plan calls for a sequence of tubes to be developed at 60 and 110 GHz, culminating in the development of a 110-GHz, 1-MW (cw) tube in 1989. If the physics of ECRH heating does not require tunable microwave sources, these tubes (or tubes requiring less demanding technology) will be sufficient for the TMPR. Should tunability be found necessary, however, some other wave source will be needed. The free-electron laser is tunable over a wide range of frequencies; it also has a fairly high theoretical efficiency at very high frequencies (> 300 GHz), perhaps making higher harmonic heating feasible. However, both the current FEL development program and experimental efforts are modest. Should tunability appear desirable, a more vigorous FEL development program will be needed.

2.3.6.3. Magnets. The development of high-field superconducting and normal conducting coils is necessary to achieve the performance level required of the TMPR. Conductor of NbTi will be used in the central-cell coils, and both NbTi and Nb_3Sn conductor will be used in the end-cell magnet coils. The central-cell on-axis field strength of 5 T can be produced by coils of NbTi superconductor, as can the required fields in the Yin–Yang anchor. This technology is well in hand, as demonstrated with the successful operation of the MFTF-A Yin–Yang magnet. Demonstration of the use of Nb_3Sn conductor at fields up to 12 T in a solenoid magnet is currently being pursued in the high-field test facility at LLNL. Such a program is one of the necessary steps in developing the TMFR 20-T hybrid coils. The Nb_3Sn conductor will have to operate at fields near 12 T. A magnet development need that is not currently a formal part of the fusion program plan is the development of the copper insert coil for use in hybrid magnets scheduled to operate in fields exceeding 12 T. Smaller versions of such coils have been operated

at the Bitter National Magnet Lab at MIT. Issues that must be addressed are strength, cooling, and fusion neutron damage. General Dynamics is presently studying similar coils in support of the MARS study. To ensure that these copper coils are ready for use in the axicell version of MFTF-B and that the technology is available for the next planning stage of the TMPR, the fusion program must develop and demonstrate the coils by 1986.

2.3.6.4. Direct Conversion. Because mirrors are inherently lossy, it is helpful to improve power balance by converting the power in the stream of plasma particles, leaving the ends of the machine into electrical power. This direct-conversion process is efficient (> 50%). Some people even suggest that direct conversion will be the primary method of extracting plasma energy for reactors using advanced (neutronless) fuels. Direct conversion of the unneutralized beam in the beamline of a neutral beam injector is possible and will be used to increase its overall efficiency. To date, LLNL's progress in the development of direct converters has been impressive. In a 1979 test a plasma direct converter was subjected to a heat flux of 70 W/cm^2 for 70 h at an energy of 100 keV and a power of 6 kW. A single-stage converter was used to convert the power of the monoenergetic charged particles to electricity at an efficiency of nearly 80%, and no noticeable degradation of collector material was reported. One year later, a plasma direct converter was successfully tested on TMX, where it collected charged particles at an efficiency of 48%. The lower efficiency in this case was due to the energy spread of collected particles.

The development plan for plasma direct conversion is directed toward increased power-handling capability. According to plan, the PDC facility will be upgraded in 1984 to handle 100 kW of power, including steady-state cryopumping. The plan calls for a 1-MW PDC facility to be built and operated by 1986. This device should produce the heat flux that would have to be withstood in the TMNS. Subsequent data on the performance of the PDC in TMNS would be obtained in time for use in the production reactor.

2.3.6.5. Vacuum Pumping. The requirements for vacuum pumping in tandem mirrors are demanding because of the large throughputs of gas from neutral beamlines, plasma flow to the direct converter, and halo plasma that have to be removed in a steady-state manner. A rapid-cycling, vacuum-pumping technique is being developed at LLNL. A test of this technique has already begun and will hopefully demonstrate technology applicable to TMNS and to the TMPR. Integrated vacuum systems tests will be performed in 1987 with D_2 and in 1988 with T_2, allowing sufficient time for use with the TMPR.

2.4. Comparison of TMPR and Future Tandem Mirrors

2.4.1. Introduction

In Section 2.3.2. we compared the requirements of the TMPR and what has currently been achieved by experiment. The result of this comparison suggests that the extrapolation of current capability is large (factors of 10^2 to 10^4) to reach the operating regime required for a production reactor. It is illustrative, therefore, to compare the parameters of MFTF-B and the fusion power demonstration (FPD) devices to those required for the TMPR. The MFTF-B, the next experiment after TMX-U, is intended to demonstrate tandem mirror operation with thermal barriers on a larger scale than was demonstrated for TMX-U. The FPD is the tandem mirror embodiment of the engineering test reactor (ETR), producing no net electricity. We will show that the MFTF-B achieves parameters that are, at most, a factor of 5 to 10 less than those of the TMPR, and that the parameters of the FPD Phase-II (D–T-burning) machine are very similar to those of the TMPR. In fact, with fairly modest changes in either baseline, the FPD could be converted into the TMPR.

2.4.2. Comparison of TMPR and MFTF-B

The first two columns of Table X show a comparison of the TMPR and the MFTF-B. The most notable difference between the two is the much lower central-cell magnetic field strength in MFTF-B. Since fusion power scales as $\beta^2\beta^4$, the effective power density in the plasma is much lower than in TMPR, even though MFTF-B has a 20% higher beta value. Extrapolations of other parameters from MFTF-B to the TMPR are not nearly as drastic as extrapolations from TMX or TMX-U. The electron and ion temperatures must increase about a factor of 3, and the ion confinement ($n\tau$) and ion density must both increase a factor of 6, going from MFTF-B to the TMPR. As for technology requirements, the TMPR will require a maximum neutral beam energy that is a factor of 6

Table X. Comparison of TMPR, MFTF-B, and FPD Phase II

	TMPR	MFTF-B	FPD-II
L_c (m)	50.0	16.5	75.0
B_c (T)	5.0	1.0	4.7
B_{max} (T)	20.0	12.0	20.0
B_c	0.4	0.5	0.7
T_{ec} (keV)	30.0	9.0	32.0
N_c (cm^{-3})	3×10^{14}	4.8×10^{13}	4×10^{14}
$(n\eta)_c$ (s/cm^3)	3×10^{14}	5×10^{13}	4.5×10^{14}
$E_{inj,max}$ (keV)	475.0	80.0	475.0
ω_{max} (GHz)	70–100	56.0	70–100
P_{fus}	400.0	0.126 (equivalent D–T)	400.0
Γ (MW/m^2)	1.9	3.9×10^{-3}	1.75
Q	4.0	0.4 (equivalent D–T)	4.75

higher than that for MFTF-B. The ECRH system for the TMPR must operate at frequencies from 30 to 100% higher than those for MFTF-B, with single-tube output powers of 1 MW, a factor of 5 larger than MFTF-B sources.

2.4.3. Comparison of TMPR and FPD

If we compare the first and third columns of Table X, we see, except for the central-cell length and beta value, that the gross characteristics of the TMPR and FPD are quite similar. They require the same maximum magnetic field strength (B_{max}), have essentially the same beam and ECRH requirements, and produce about the same neutron wall loading (Γ) for roughly the same power investment (P_{fus}/Q). These similarities suggest that a slight redefining of the TMPR, particularly lengthening of the central cell, will define a route by which the FPD could be converted to a TMPR. The obvious advantages are that the existing fusion driver could be used and that only the power-producing blanket modules would have to be replaced by materials-producing modules.

3. TOKAMAK FUSION DRIVER

3.1. Design Requirements

The requirements set forth in this subsection are derived from objectives discussed in the introduction to this volume and elsewhere in the respective volumes. Subsequent parts of this section describe how the requirements are satisfied in a particular tokamak embodiment called TORFA-D2. Many of the fusion driver engineering features of TORFA-D2 are similar to those of the FED-R,[31] a test reactor concept studied at the Fusion Engineering Design Center at Oak Ridge and, in turn, based on the TORFA concept proposed in 1980.[32]

3.1.1. Required Nuclear Capability

a. The fusion neutron wall loading, averaged over the plasma chamber wall, must exceed 1 MW/m^2 with pulse lengths of at least 1000 s and a duty factor of at least 90%.
b. Production blankets must cover as close to 100% as possible of the plasma chamber wall.
c. At least 75% of the fusion neutrons must penetrate the wall of the plasma chamber without scattering.
d. The region dedicated to production blankets must have a depth of at least 0.8 m completely surrounding the plasma chamber.
e. The fusion power output must be in the range 350–500 MW.

3.1.2. Fusion Plasma Requirements

a. The electron and ion temperatures, energy-confinement time, and permissible impurity-ion concentration in the D–T plasma are to be selected at levels needed to generate a fusion neutron wall loading of 1.5 MW/m^2 at the largest practicable fusion energy Q_p.
b. The ratio of plasma pressure to magnetic field pressure (β) is to be the maximum value consistent with presently known MHD stability limitations, as derived from the the-

oretical analysis buttressed by existing experimental data.

c. The plasma current must be adequate to support the energy confinement time (τ_E) and β value that satisfy requirements a and b above, as dictated by present theoretical and empirical understanding of the dependencies of τ_E and β on plasma current.

3.1.3. Selection of Plasma Heating Method

a. The principal method chosen for plasma heating must be a proven technique.

b. The principal plasma heating method must also be capable of driving the plasma in the steady state.

c. Auxiliary heating methods to be used for startup or profile control must require injection of no more than one-tenth of the injected power of the principal heating method.

3.1.4. Magnetics Requirements

a. The toroidal field (TF) coils are to make use of proven technology for the construction of large magnets.

b. The shape and demountability features of the TF coils must be chosen to facilitate the installation and removal of the production blankets.

c. Normal-conducting TF and PF (poloidal field) coils are to be cooled with pressurized water.

d. The TF coils, if normal-conducting, must consume no more than 300 MW of electrical power at full design field.

e. The insulation in the TF coils must be capable of at least 10^{12} rads of nuclear radiation without incurring significant damage.

f. The configuration, conductor type, and dimensions of the PF coils are to be chosen for minimal power dissipation, consistent with the need to maintain the plasma shape and divertor separatrix.

g. PF coils located in the bore of the TF coils must have demountable joints to permit replacement.

h. The OH (ohmic-heating) solenoid must deliver at least 10 Wb of flux change.

i. Power dissipation in the OH solenoid must not exceed 10 MW during the plasma burn phase, which begins ~ 20 s after initiation reactor startup.

3.1.5. Plasma Startup and Operational Requirements

a. Steady-state operating values of plasma current, ion and electron temperatures, and fusion neutron production are to be attained by 20 s after initiation of startup.

b. Dependence on an OH solenoid for current maintenance is to be minimized.

c. See requirement 3.1.3.c.

d. Pellet injection is to be used as needed to help neutral injection and recycling maintain the required D and T concentrations in the plasma.

3.1.6. Impurity and Particle Control Requirements

a. A single-null poloidal divertor is to accomplish all impurity control and particle removal.

b. All vacuum-vessel pumping is to be carried out through the divertor ducts and neutral beam ducts.

c. The divertor is to be modularized to facilitate replacement of its hardware components subject to erosion.

d. Protective plating on director components and on the nearby plasma vessel wall should be fabricated of beryllium whenever possible.

3.1.7. Vacuum-Vessel Requirements

a. The chamber containing the fusion plasma is to serve as the "hard" vacuum boundary.

b. The resistance of the vacuum vessel in the toroidal direction must permit full plasma startup in 20 s or less.

c. The vessel must be sufficiently rugged to avoid substantial harm in the event of a major plasma disruption (loss of all plasma current).

d. The vessel coolant system must be capable of removing a steady-state thermal loading of 70 W/cm^2 with a power consumption of no more than 30 MW.

e. The vessel wall is to be "neutronically thin." See requirement 3.1.1.c.

3.1.8. Availability and Maintenance Requirements

a. The TORFA-D2 subsystems must be available often enough to permit an annual capacity factor of at least 70% for the plant.
b. A damaged TF coil must be replaceable in two months or less.
c. Divertor modules must be removable without disturbing the TF or PF coils.
d. The radiation dose level, if any, at the TF coil joints must be low enough at 48 h after shutdown to permit hands-on disassembly and reassembly of the joints.
e. Access to vacuum-vessel sector joints and duct interface ports is required for leak detection and repair.
f. A damaged vacuum-vessel sector must be replaceable in no more than two months.
g. Personnel access to the outside of the reactor must be permissible at 48 h after shutdown.
h. Rapid access to the service connections on blanket ducts is required.
i. Neutral-beam-injector ion sources must be readily available for replacement.

3.2. Design Description

3.2.1. Overview

The tokamak embodiment that satisfies the requirements set out in Section 3.1. is called TORFA-D2. Table XI lists the basic fusion system parameters of TORFA-D2, and Figs. 21 and 22 show elevation and plan views. Figure 23 illustrates the relative sizes of TORFA-D2 and TFTR.[33] The TORFA-D2 device

Table XI. Fusion System Parameters for Tokamak Production Reactor TORFA-D2

Geometry	
Plasma major radius, R_p (m)	3.9
Plasma minor radius, a_p (m)	0.95
Plasma elongation, D-shaped	1.5
Plasma aspect ratio (A)	4.1
Plasma volume (m^3)	93.0
TF coil inboard leg, major radius (m)	2.0
TF coil bore, nearly rectangular (m)	4.5×6.75
Vacuum-vessel bore, racetrack-shaped (m)	2.3×4.3
Inboard blanket and shield thickness (m)	0.8
OH solenoid outer radius (m)	0.75
Divertor chamber height (m)	1.1
Magnetic systems	
TF coil type	Normal conducting copper plates
TF coils	12.0
Maximum TF coil power dissipation (MW)	220.0
Maximum toroidal field at conductor (T)	9.8
Maximum toroidal field on plasma axis (T)	5.0
TF coil coolant	pressurized water
TF ripple at plasma edge (%)	0.9 peak to average
TF ripple on plasma axis (%)	0.1
PF coils inside bore of TF coils	
Type	Normal conducting copper turns
Coolant	pressurized water
Number	1 top, 3 bottom
Power dissipation (MW)	50.0
Power coils outside TF coils	
Type	NbTi, superconducting
Coolant	Liquid helium, 5 K
Number	2.0
Magnetic systems	
OH solenoid type	Bitter plate
Maximum field in solenoid (T)	9.5
Maximum flux swing from solenoid (Wb)	13.0

Table XI. *Continued*

Plasma heating systems and startup	
Ionization and preheating	
RF frequency (GHz)	93.0
RF power (MW)	2.0
RF pulse duration (s)	1.0
Flux swing in OH solenoid (Wb)	≥ 10.0
Flux swing in EF available for startup (Wb)	≥ 12.0
Neutral beam energy, E_b (keV)	250 (D^0) and 340 (T^0)
Injectors	4 D^0 and 2 T^0
Neutral beam power, P_b (MW)	150 (25 per injector)
Beam injection angle from perpen	40 for D^0
dicular to plasma surface (degrees)	30 for T^0
Plasma operating characteristics	
Plasma current, I_p (MA)	5.5
Safety factor, q	2.4
Electron density (cm^{-3})	$1.5[1-r^2/a^2]\times 10^{14}$
Electron temperature (keV)	$20[1-r^2/a^2]^2$
Ion temperature (keV)	$38[1-r^2/a^2]^2$
Volume-averaged total β	0.06
Fraction of total pressure in hot ions	1/3
Energy-confinement time (s)	0.35
$\bar{n}_e\tau_E$ ($cm^{-3}s$)	3×10^{13}
Effective charge, Z_{eff}	1.5–2.0
Pellet injection	Tritium, 10 s^{-3} s, 3-mm diam, v = 2000 m/s
Particle and impurity control	Single-null poloidal divertor
Fusion burn characteristics	
Fusion power density (MW/M^3)	4.8
Total fusion power (MW)	450.0
Fusion α power (MW)	90.0
Neutron wall loading (MW/m^2)	
Spatially averaged	1.4
Outboard wall, near midplane	1.65
Pulse length	Steady state
Downtime for restart (s)	100.0
Annual capacity factor	≥ 70.0
Thermal aspects	
Nonneutron power to first wall (MW)	130.0
First-wall thermal loading (W/cm^2)	70, spatially averaged
Thermal power to divertor (MW)	380.0
First-wall coolant	Helium at 300 psi, up to 300°C
Divertor coolant	Pressurized water, up to 150°C
Shield coolant	Pressurized water, up to 100°C
TF coil conductor coolant	Pressurized water, up to 60°C
Tritium systems	
Throughput (kCi/h)	500.0
Inventory, excluding blanket systems (MCi)	10.0
Annual consumption (kg)	18.0
Plasma vessel	
Material and construction	Stainless steel-316, double-wall
Coolant	Helium at 300 psi
Sectoring	6 radially removable sections
Protective "armor"	Graphite or beryllium coating
Hard vacuum boundary	At vessel

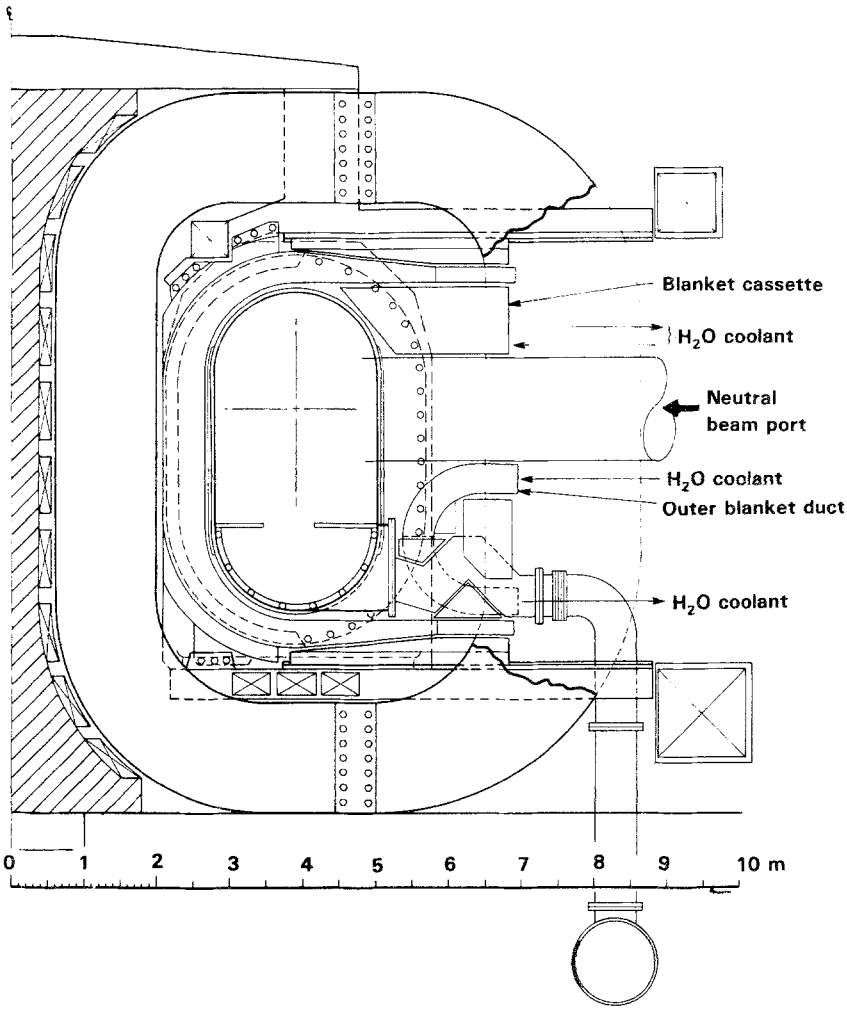

Fig. 21. Elevation view of the tokamak production reactor.

is actually a scaled-up version of FED-R. A detailed discussion of the plasma and physics subsystems of FED-R can be found in Ref. 31. Table XII compares the principal parameters of TORFA-D2, FED-R, TFTR, and JET. The TFTR and JET are scheduled to start up in 1983, with full operation by 1986.

Reference 1 discusses the reasons for selecting $Q_p = 3$ as the fusion energy amplification for TORFA-D2. In what follows we briefly describe the rationale for choosing the key fusion technology components. Subsections 3.2.2. through 3.2.5. which follow, describe the major technology components in more detail.

3.2.1.1. Toroidal Field Coils. Resistive TF coils were chosen for three reasons: (1) TORFA-D2 must be deployable in the 1990s and have a high probability of successful operation. (2) There are many uncertainties about our ability to completely shield superconducting coils in *compact* toroidal devices from intense radiation fields. (3) The TF coils should be demountable, which is not possible with superconducting windings.

If the TF coils are massive enough, they can be operated steady state at the precribed magnetic field, with a resistive power loss in the range 220–250 MW. To enhance access for replacement of all the in-bore components (e.g., vacuum vessel sectors, PF coils, and materials production blankets), demountable joints are included in the upper and lower segments of the TF coils. The demountable joints also make it feasible to replace a damaged TF coil in a reasonable time—a problem that has not been resolved in super-

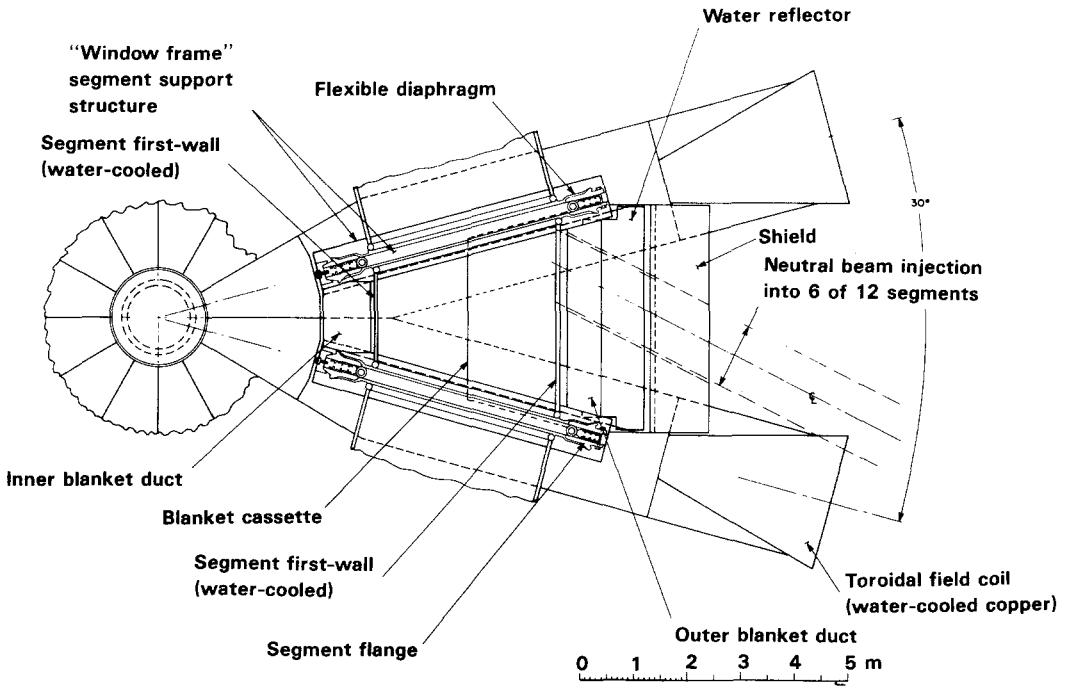

Fig. 22. Plan view of the tokamak production reactor.

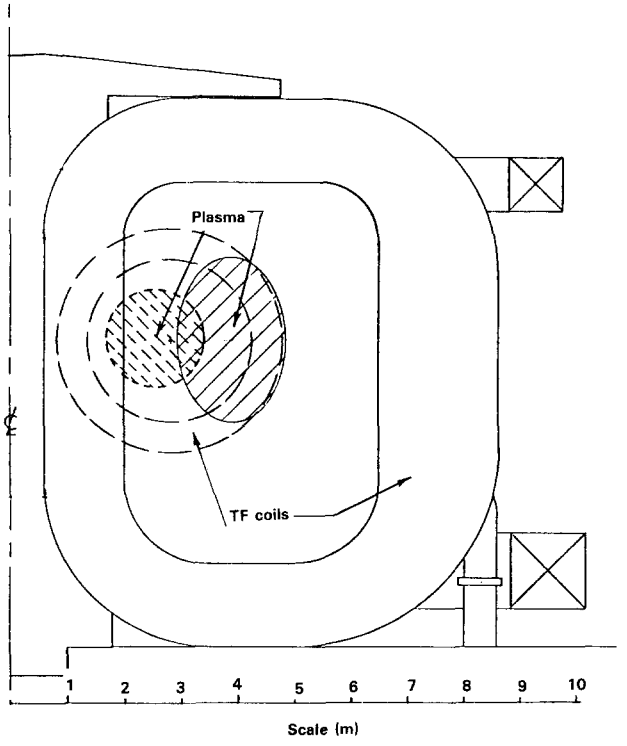

Fig. 23. Size comparison of TORFA-D2 (solid lines) and TFTR (dashed lines).

conducting-coil tokamak reactor concepts. As discussed in Section 3.4. the demountable joints also make conversion of a near-term test reactor (such as FED-R into TORFA-D2) rather straightforward.

3.2.1.2. Poloidal Field Coils. Whenever possible, PF coils should be located external to the TF coils for ease of maintenance and replacement in the event of failure. About 80 MW of resistive power loss can be avoided by using superconductors in place of normal conductors for the external "ring coils." The two reasons why superconducting coils can be used with confidence in this application, but not for the TF field, are (1) the absence of a significant nuclear radiation field in the location of the external ring coils and (2) the relatively low maximum magnetic field and relatively simple forces on the coils.

3.2.1.3. Neutral Beam Injection. This system was chosen as the primary plasma heating system for four reasons: (1) The largest plasma temperatures and highest β values to date have been achieved with neutral beam injection, (2) theoretical analyses indicate that the same beam systems can be used for plasma heating and current drive,[34] (3) beam-target reactions enhance fusion reactivity, (4) a larger stable plasma pressure may be attainable if a significant

Table XII. Comparison of Principal Parameters of Tokamak Fusion Drivers

	TFTR mid-1980s	FED-R2[a] early 1990s	TORFA-D2 late 1990s	JET mid-1980s
Major radius (m)	2.5	3.5	3.9	2.95
Minor radius (m)	0.85	0.85×1.3	0.95×1.45	1.25×2.1
Maximum B at coil (T)	9.5	7.0[b] 8.8[c]	9.8	7.0
Maximum B at plasma axis (T)	5.2	4.0[b] 5.0[c]	5.0	3.5
Plasma current (MA)	3.0	3.6[b] 4.4[c]	5.0	5.0
Neutral beam energy (keV)	120.0	150.0[b]	250 (D^0) 340 (T^0)	160.0
Neutral beam power (MW)	30.0	50.0[b]	150.0	25.0
$n_e\tau_E$ (cm^{-3} s)	$\sim1\times10^{13}$	$\sim2\times10^{13}$	$\gtrsim3\times10^{13}$	$\gtrsim3\times10^{13}$
$\langle\beta\rangle$ = plasma pressure magnetic field pressure (%)	3.0	5.0[d]	6[d]	5.0
Pulse length (s)	~1.0	⩾1000	Steady state[e]	10.0
Duty factor	0.003	⩾0.25	⩾0.90	0.02
Fusion gain, Q_p	~1.0	1.5[b]	3.0	>1.0
Fusion power (MW)	20.0	75.0[b]	450.0	> 25.0
Uncollided neutron wall loading (MW/m^2)	0.2	0.4[b]	1.4	≃0.2
Electrical power consumption (MW)	660.0 (short pulse)	405[b]	575.0	650.0

[a]Proposed test reactor under conceptual design at FEDC (Ref. 29).
[b]Values given are for Stage I operation.
[c]Maximum design values.
[d]Approximately 2/3 of the pressure is in bulk plasma and 1/3 is in superthermal (injected) ions.
[e]Assuming that steady-state, noninductive current drive is feasible.

fraction of the pressure resides in superthermal ions. The fourth reason is important when fast ions contribute notably to fusion power production, which may be the case when $Q_p < 3$.

3.2.1.4. Magnetic Divertor. Either a magnetic divertor or a "pumped limiter" can, in principle, be used to control the densities of reacting particles and impurity ions, as well as for the disposal of thermal flux from the plasma. The effectiveness of the poloidal magnetic divertor has been verified in a number of tokamak experiments,[35] while the effectiveness of its principal rival—the bundle divertor—remains dubious. Although the pumped limiter would be simpler and less costly to incorporate, serious doubts remain about its ability to withstand erosion from plasma bombardment over a significant time. Sputtering in a divertor chamber can be isolated from any effect on the plasma, but material eroded from a limiter in the main torus could seriously degrade the reacting plasma. Hence, in the absence of proven, long-time, pump-limiter operation, a single-null poloidal divertor has been selected for TORFA-D2.

3.2.1.5. Remote-Maintenance Systems. Remote-maintenance methods for the TORFA-D2 components are discussed in Ref. 2.

3.2.2. Magnetic Systems

The TORFA-D2 magnetic systems consist of 12 copper TF coils, 4 copper internal PF coils, 2 superconducting external PF coils, and 1 copper OH solenoid. The copper coils are water-cooled, although the OH solenoid can be cooled with liquid nitrogen, which would permit one to obtain a larger flux swing from this solenoid.

3.2.2.1. TF Coils. Figure 24 shows a cutaway view of the TF coils, each of which consists of about 20 plates insulated by SPINEL (magnesium aluminate). The plates are assembled from subplates, using permanent lap joints. All plates are connected in series by the type of electrical joint illustrated in Fig. 24. The water-coolant channels are slots milled into the sides of the plates. Demountable mechanical

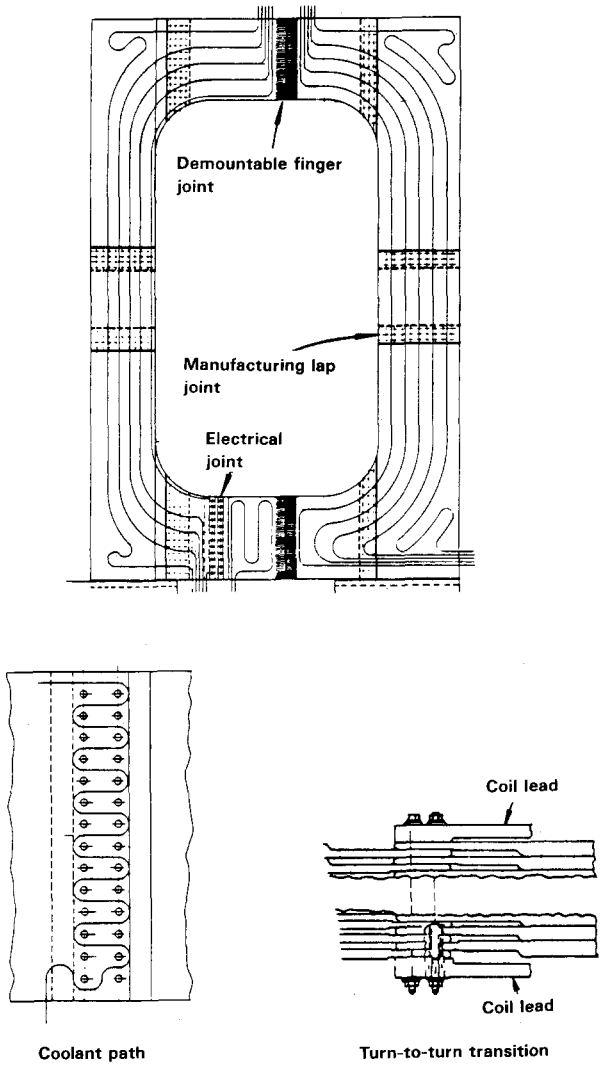

Fig. 24. Details of toroidal field coil for TORFA-D2.

finger joints are located in the upper and lower arms of the TF coils. Figure 25 shows the details of one of the demountable finger joints, which is similar to that used in the Doublet III device at General Atomic Company. The in-bore shielding is sufficient to allow the joints to be disassembled by contact maintenance. About 140 h are needed to disassemble one joint, while reassembly would take about 225 h.[36] However, the two joints of a single coil can be dissembled simultaneously; given enough crews, many TF coils could be disassembled simultaneously if required.

The SPINEL insulator can be applied by plasma arc spraying. This insulation material can withstand an irradiation dose of at least 10^{12} rads before its mechanical or electrical properties become significantly degraded.[37]

Figure 26 shows the coil case and intercoil support structure needed to counteract overturning moments on the TF coils. The copper plates themselves are self-supporting against the in-plane magnetic forces.

3.2.2.2. PF Coils. The internal copper coils have many turns that are held together by bolted joints.[31] Each coil has three joints located at 120° degree azimuthal separations. These joints have low resistance, but reassembly is tedious and requires remote equipment.

3.2.2.3. OH Solenoid. Figure 27 shows the OH solenoid configuration and its major engineering parameters. The solenoid is constructed of water-cooled Bitter plates, as in the Alcator devices at MIT. The 13-Wb flux swing provided by the solenoid is needed only during the current startup phase (see Section 2.3.3.6.). To minimize resistive power loss during the quasi-steady burn, the solenoid current is programmed to zero during the first 100 s of the power pulse, with the neutral-beam-driven current compensating for the reverse emf during this process.

3.2.3. Plasma Vessel

The water-cooled wall of the plasma vessel serves as the "hard" vacuum boundary. The vessel consists of 12 sectors bolted and welded together. A detailed description of the vessel design is given in Ref. 2. (Note: Neutron wall loadings quoted in these volumes refer to the uncollided neutron power flux on this wall.)

Figure 28 shows the positions of the major auxiliary equipment that must have access to this vessel. This equipment includes the neutral beam injectors for heating and current drive, the pellet injectors for fueling, and plasma diagnostics for monitoring the plasma operating parameters and for relaying this information to the plasma control system. While a duct configuration is favored for the TORFA-D2 blankets (see Ref. 2), cassette blankets are used in those sectors to which major pieces of auxiliary equipment (such as injectors) are attached.

3.2.4. Magnetic Divertor

TORFA-D2 has a single-null poloidal divertor, with the pumping chamber located at the bottom of the plasma vessel and separated from the plasma

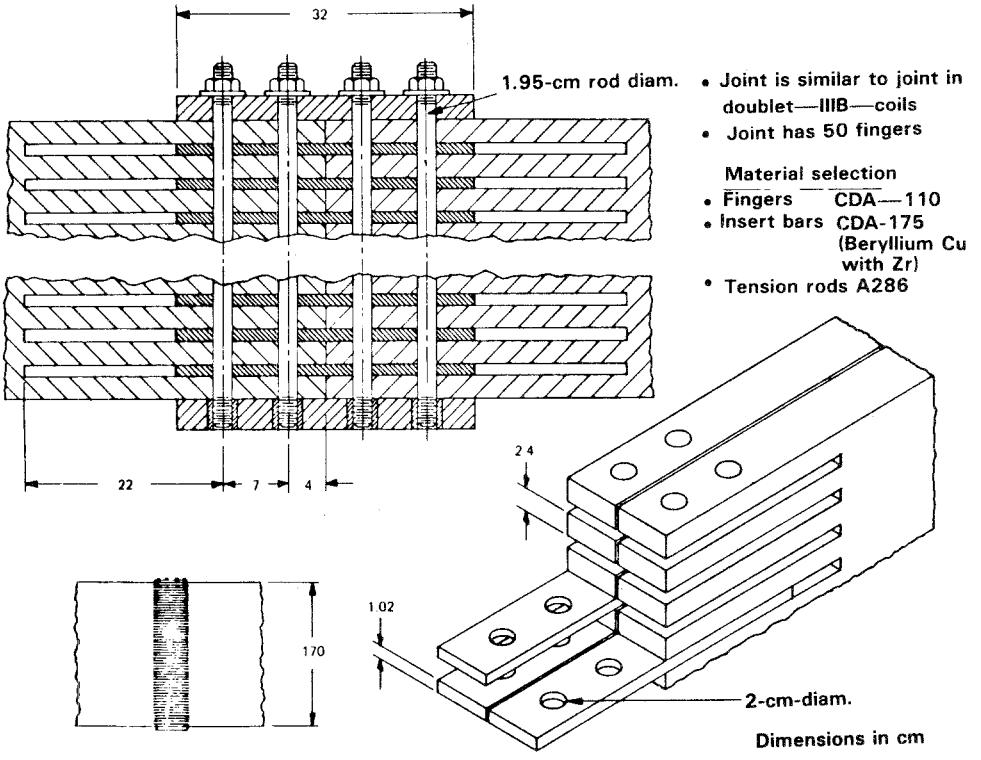

Fig. 25. Details of finger joint in toroidal field coils.

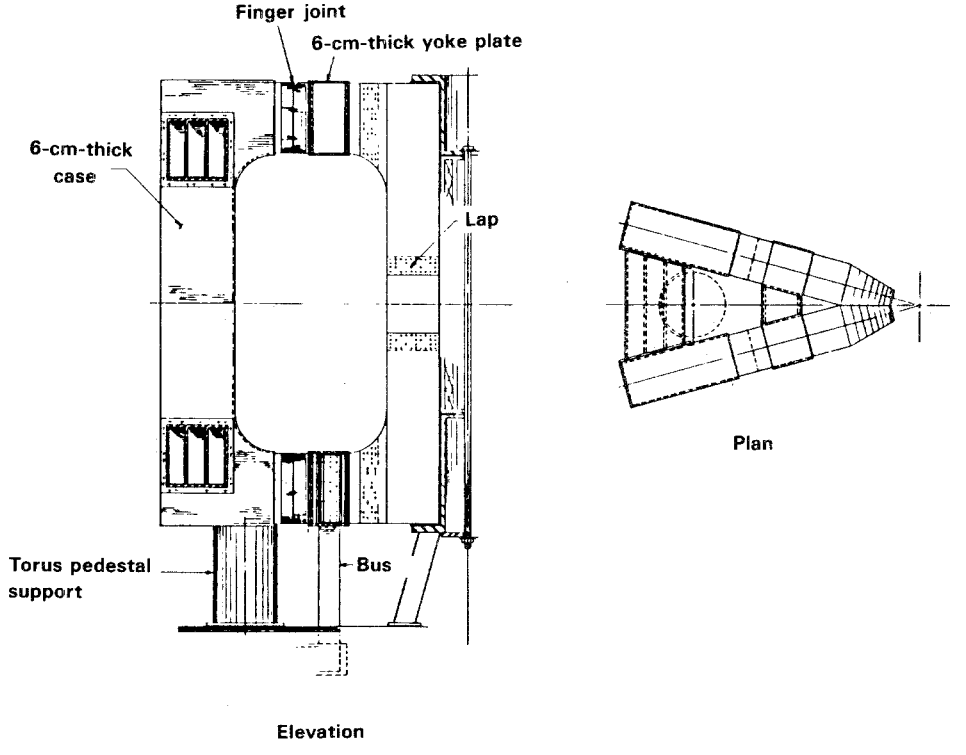

Fig. 26. Structural support for toroidal field coil.

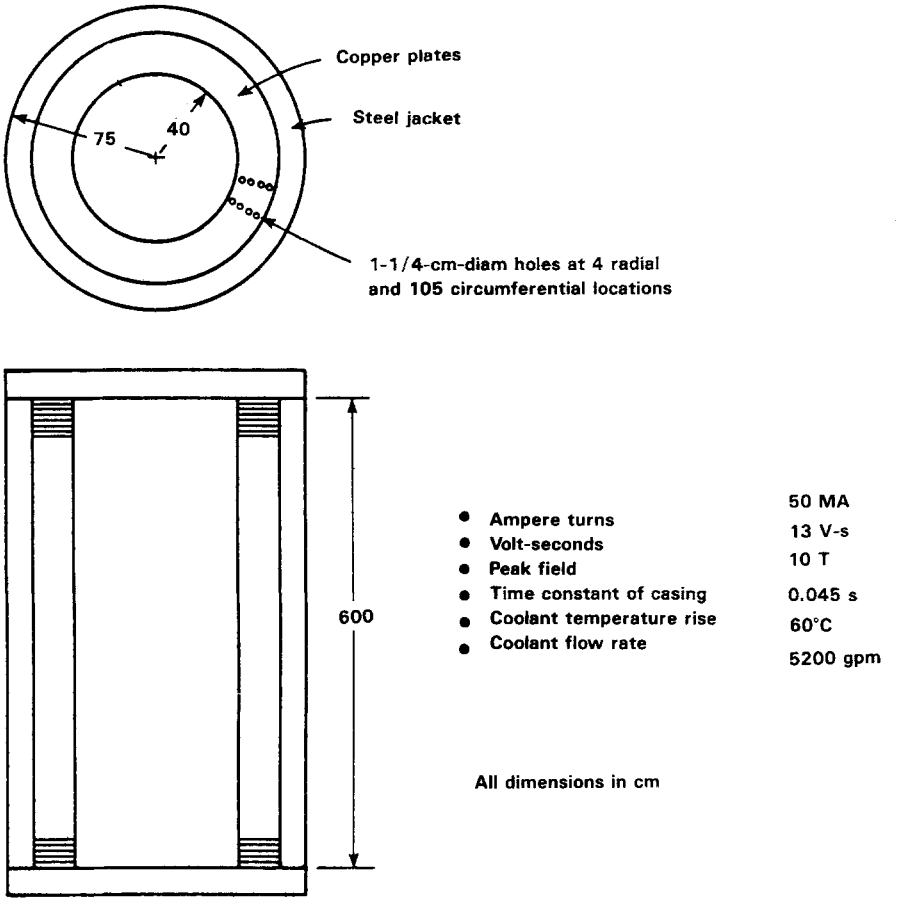

Fig. 27. Ohmic-heating solenoid of TORFA-D2.

chamber by a baffle. On the basis of present-day tokamak experiments,[35] the divertor is expected to remove 75% of the nonnuclear thermal power flowing from the plasma. All particle pumping, except for a small fraction performed by the beam injector ducts, is carried out by the divertor. The divertor chamber is comprised of 12 modules, each with its own vacuum pumping system. The internal components are water-cooled. Each module is readily removable by radial extraction when the internal components must be replaced because of severe erosion by the bombarding particles. Figure 29 indicates the module extraction motion for the case of a sector to which a neutral beam injector is attached.

Neutron attenuation in the divertor hardware can result in a significant loss of effective blanket coverage, even if the blanket extends beneath the divertor chamber. This problem can be ameliorated by using 2-cm-thick beryllium tiles as the first surface on all divertor components and on the baffle to the pumping chamber[38] to take advantage of the (n,2n) reaction in beryllium.

3.2.5. Neutral Beam Injectors

Figure 30 shows a top view of the D^--based neutral beam injector that would be used with TORFA-D2. Six ribbon beams of D^- or T^- ions are obtained from self-extracting, surface-conversion, negative-ion sources. The ions are accelerated electrostatically to 250 keV. A series of TFF (transverse-field focusing) accelerators transports the ribbon beams through the neutron shielding to the laser photodetachment neutralizer. Beam transport occurs via a series of curved paths so that there is no direct line of sight from the fusion neutrons to the ion sources or accelerators. The final TFF component directs each ribbon beam through the laser resonator to a common focus in the tokamak plasma.

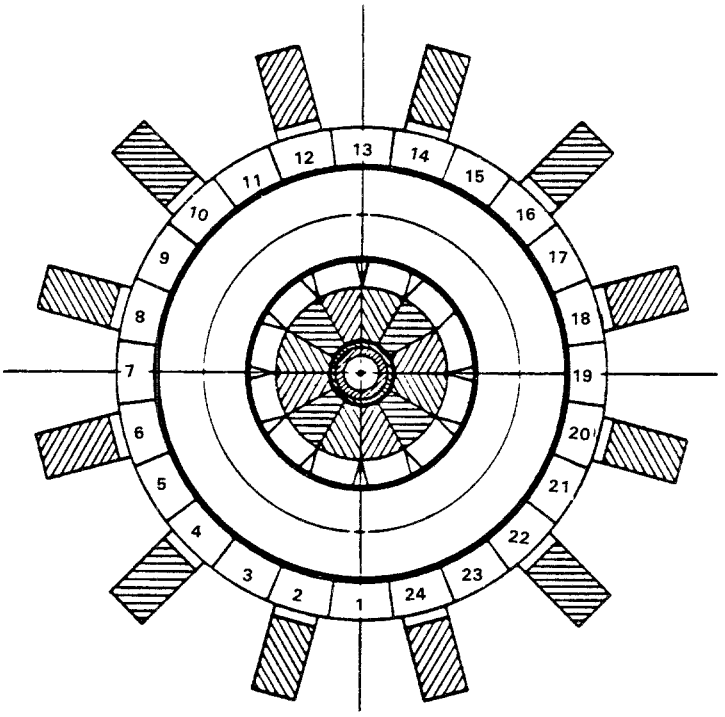

Auxiliary equipment	Position No.	Outboard blanket configuration
Heating	7 through 18	Cassettes
Fueling	13 and 17	Cassettes
Plasma diagnostics	1 and 11	Cassettes
None	2 through 6 19 through 24	Ducts

Fig. 28. Positions of major auxiliary equipment in TORFA-D2.

The negative-ion source is under development at Lawrence Berkeley Laboratory; to date, it has produced more than 1 A of D− current in multisecond pulses,[26] compared with the 20 A required for the TORFA-D2 injector. The TFF accelerator has been used successfully with electrons and is being adapted for ion beam acceleration at LBL. The oxygen-iodine chemical laser for photodetachment has been developed for the Air Force Weapons Laboratory and at TRW. A neutralization efficiency of 97% is expected with this type of laser. LBL plans to operate a prototype of this type of neutral beam by the late 1980s.

The injection angles for the beams are chosen so that the entire 5.5-MA plasma current can be driven by the injected fast ions when $Z_{\text{eff}} \simeq 1.5$. First-order neutronics analyses indicate that the injector ducts will reduce the total breeding ratio in the TORFA-D2 blankets by roughly twice the ratio of the duct cross-sectional area in the torus wall, or about 4%.

3.2.6. Device Operation

The sequence of operations of a typical fusion pulse in TORFA-D2 is as follows: The TF coils are

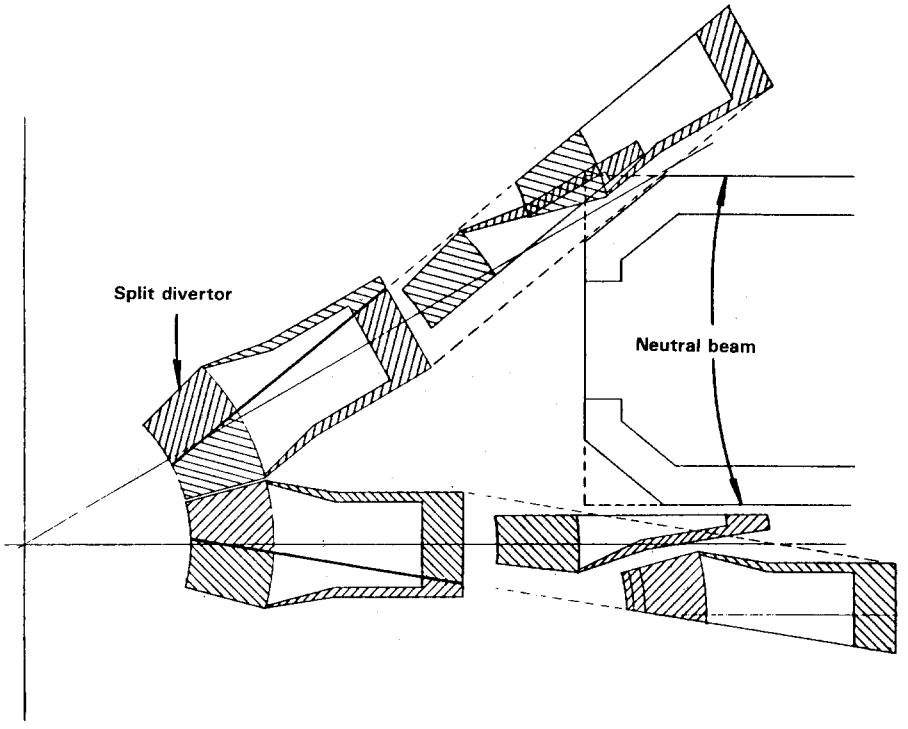

Fig. 29. Retraction of divertor module.

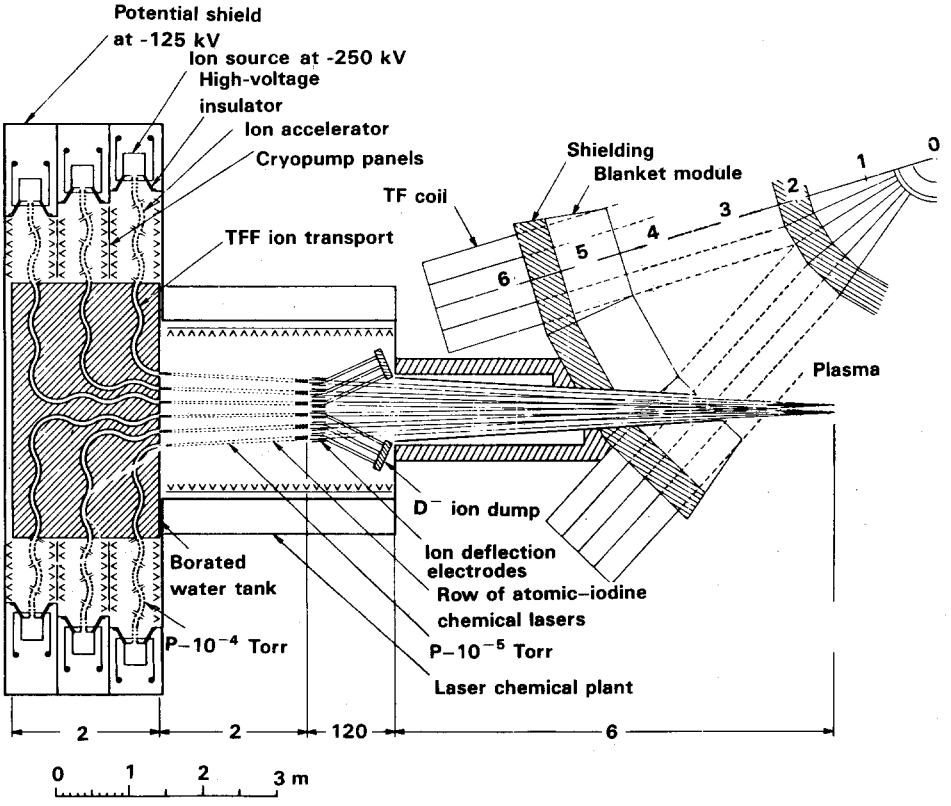

Fig. 30. Negative-ion-based neutral beam injector.

generally operated at constant current. By contrast, the currents in the PF and divertor coils undergo large changes at the beginning and end of the pulse and may vary slightly during the pulse as a consequence of changes in plasma position, pressure, or current. If neutral beam current drive is successful, each pulse can be tens of thousands of seconds is duration.

The plasma current (I_p), density (n_e), and temperature (T_e or T_i) are to be increased by a series of processes with a total duration of about 15 s. The flux linkage from the OH solenoid and the equilibrium field (EF) coil system at the plasma major radius (3.9 m) does not fully satisfy the flux-linkage requirements for a full-current startup (5.5 MA). Hence, it must be supplemented by neutral beam current drive during startup. A line-averaged density of at least 2×10^{13} cm^{-3} is needed to trap the injected neutral beams, and an I_p of at least 300 kA is needed to provide adequate orbit confinement of the energetic ions formed from the beams. This density and current are produced in 2 s or less by first pre-ionizing the filling gas and heating the electrons to a temperature between 10 and 50 eV by means of 2 MW of RF power at 93 GHz (electron cyclotron heating) and then by initiating the OH transformer to generate a 300-kA current while T_e is raised to about 500 eV and n_e is increased to about 2×10^{13} cm^{-3}.

One by one the neutral beams are activated. In combination with the flux linkage provided by the increasing current in the EF coils, the gradually increasing neutral beam power takes I_p to its final value of 5.5 MA in about 15 s. Simultaneously, the beams heat the plasma electrons and bulk ions to their operating values of T_e and T_i. The injected beams maintain I_p, T_e, and T_i throughout the burn pulse. Only the four D^0 beams are needed to drive I_p, and their efficiency is estimated to be 0.06 A/W. The two T^0 beams are injected at a steeper angle and thus, for adequate penetration, require an energy of about 340 keV rather than the usual $1.5\times E_D$.

Together with recycling, the D^0 beams are adequate for fueling the deuterium component of the plasma. Injection of frozen tritium pellets (4 mm in diameter) is required to complement the fueling by the T^0 beams. During the burn, the beam power, beam voltage, and pellet injection rates are varied to keep fusion neutron output at the required level. Particle pumping and plasma heat removal are accomplished by the magnetic divertor. An almost indefinitely long fusion pulse is possible in principle.

3.2.6.1. Plasma Equilibrium. The PF coils maintain a D-shaped plasma, with a single null point defining the plasma, as indicated in Fig. 31. The outer PF coils provide most of the vertical field needed for equilibrium of the plasma column. The internal PF coils are instrumental in producing the vertical plasma elongation needed to reach the highest plasma pressure and for creating the magnetic separatrix outside of which magnetic field lines are "diverted" into the divertor chamber.

3.2.7. Total Power Requirements

Figure 32 shows the power-flow diagram for TORFA-D2. The following assumptions underlie this diagram:

1. Steady-state operation, with the plasma current being driven by the same neutral beam injectors used for plasma heating.
2. Fusion power amplification $Q_p = 3.0$ (fusion power/injected beam power).
3. Neutral beam injector efficiency = 0.55 (injected power/electrical power).
4. Spatially averaged blanket energy multiplication = 1.5.
5. Cold blankets (i.e., no electricity production).

TORFA-D2 has a steady-state electrical power consumption of 575 MW_e. In the baseline design, none of the heat flowing from the magnet systems, torus, or blankets is converted into electricity. The total rejected heat is 1205 MW, of which 560 MW is the fusion power generated and 180 MW is additional nuclear heat produced in the blankets. The electrical power required would be taken directly from the grid. Approximately 7 GJ of pulsed energy is needed during startup, mainly for the OH system. This pulsed energy requirement will be met by motor-generated flywheel sets.

3.3. Current State-of-the-Art and Development Requirements

Tables XIII and XIV summarize the major plasma-physics and technological uncertainties identified in attempting to implement the TORFA-D2 fusion driver. The more important unresolved issues are discussed below.

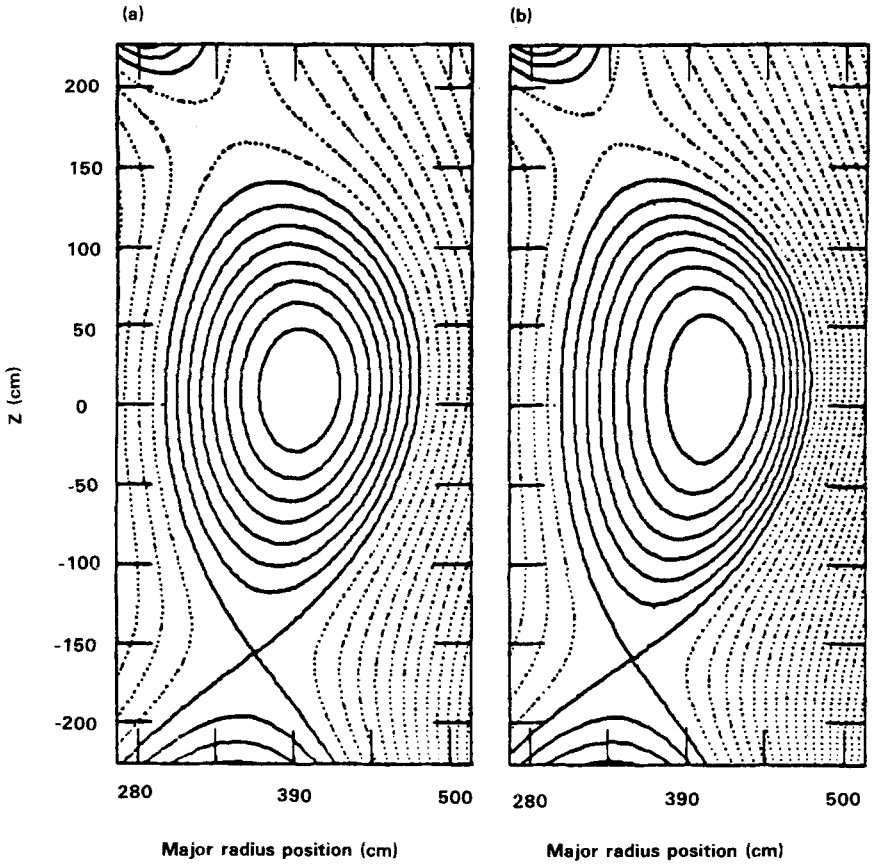

Fig. 31. Elevation view of magnetic flux surfaces of TORFA-D2 plasma.

3.3.1. Major Plasma Physics Uncertainties

1. The main advances that must be made beyond anticipated TFTR performance in the mid-1980s ($Q_p \sim 1$, with ~ 0.003 duty factor) revolve around the attainment of high duty factor, preferably $Q_p \sim 3$, and neutron wall loading $\simeq 1.5$ MW/m^2. These requirements demand operation at moderately large $n\tau_E$ and at high plasma temperatures and β (plasma pressure/magnetic pressure).
2. The uncertainty in plasma current drive by neutral beams or RF waves at high plasma density will be addressed. Near-term research programs will be carried out on many tokamaks and, at very high power, on TFTR and JET in the late 1980s.
3. Relevant research programs to address the uncertainty in establishing and maintaining $\langle\beta\rangle = 4\%$ for the bulk plasma and 2% for superthermal (injected) ions are currently being carried out on PDX and D-III. In the mid-to-late-1980s programs at higher fields and with greater heating power will be pursued on D-III Upgrade and other tokamaks capable of plasma-shaping.
4. Relevant confinement experiments attempting to achieve $n_e\tau_E \simeq 3\times10^{13}$ cm^{-3} at high plasma temperature and high beta will be carried out on TFTR, JET, and D-III Upgrade in the mid-1980s.
5. The capability for removing 240 MW of nonnuclear heat flowing from the plasma in steady-state operation while maintaining plasma ion purity and the prescribed radial profiles of T_e and T_i must be developed. Long-pulse operation in TFTR, JET, and JT-60 in the mid-to-late-1980s will address this issue, but at a power level that is an order of magnitude smaller. Relevant technology development will be carried out in ex-reactor test facilities.

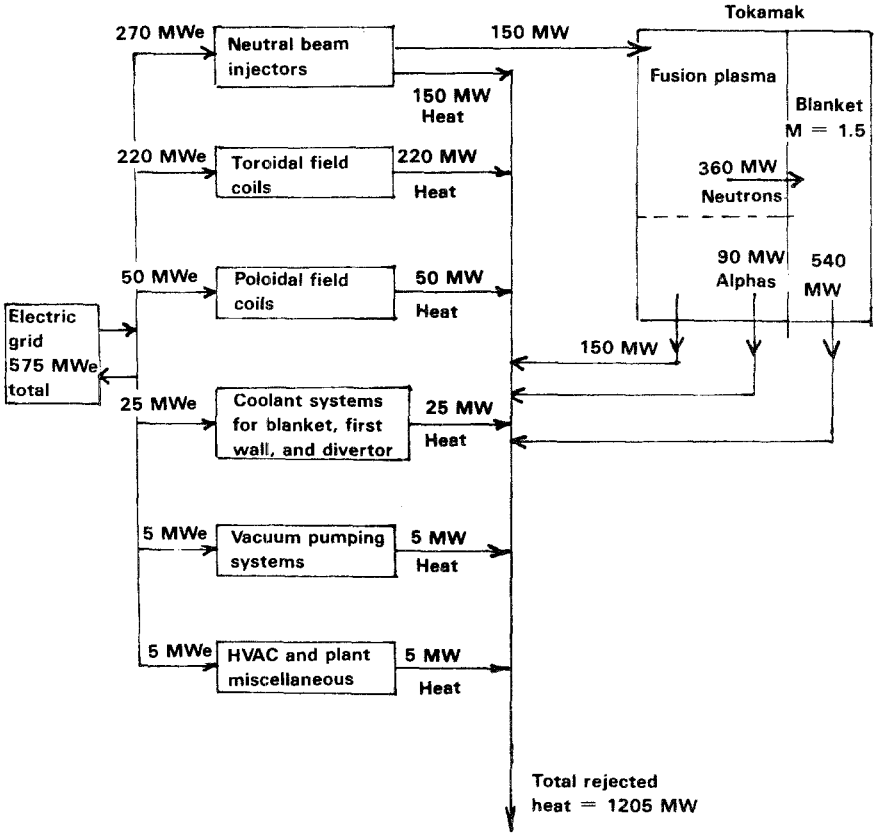

Fig. 32. Power-flow diagram for TORFA-D2.

3.3.2. *Consequences of Inability to Meet Physics Requirements*

An examination of Table XIII reveals that the three major potential stumbling blocks to achieving the specified plasma-physics operation in TORFA-D2 could be difficulties in the following:

1. Control of major plasma disruptions at high β.
2. Achievement of high $\bar{n}_e\tau_E$ at high β.
3. Achievement of steady-state current drive.

Major plasma disruptions must be minimized to eliminate potential damage—caused directly by the disruption (e.g., through erosion or arcing) and indirectly through fatigue—to the vacuum vessel and other reactor components. High $\bar{n}_e\tau_E$ is required to achieve high Q_p and to permit smaller neutral beam power for a given fusion neutron production rate. If β must be limited to eliminate major plasma disruptions or to retain high $n\tau$, the following consequences result:

1. The neutron production rate for a given B will be reduced as β^2.
2. The capacities and costs of certain subsystems (e.g., neutral beam injectors, tritium-handling equipment, vessel and divertor coolant systems, and some electrical power systems) will be reduced as β.
3. The production cost per fusion neutron will vary approximately as $\beta^{-1.5}$.
4. Achievement of a 450-MW fusion power production will necessitate going to a larger reactor or a higher magnetic field.

The inability to achieve steady-state noninductive current drive will result in fusion pulse lengths in the range 500–1000 s and in a duty factor of 88–94%. It will also have the following consequences:

1. The OH primary windings must be placed in the bore of the TF coils to increase the cross section of the transformer core. The major

Table XIII. Plasma-Physics Status and Requirements for the TORFA-D2 Fusion Driver

	Present performance	Required performance	Means of demonstrating required performance
$\langle\beta\rangle$ = plasma pressure/ magnetic pressure (%)	0.045 at low T_e and τ_E	0.06	D-III Upgrade 1986–88 JET late-1980s
$n_e\tau_E$ at high temperature and moderate $\langle\beta\rangle$	5×10^{12} cm^{-3} s at $T_i = 12$ keV and $T_e = 6$ keV at $\langle\beta\rangle \simeq 0.015$[a]	3×10^{13} cm^{-3} s at $T_i \sim 30$ keV and $T_e \sim 20$keV at $\langle\beta\rangle \simeq 0.06$	1×10^{13} cm^{-3} s at $T_i \sim 20$ keV and $t_e \sim 10$ keV in TFTR and JET in mid-1980s, with $\langle\beta\rangle \gtrsim 0.03$
Ion temperature, T_i(O) (keV)	12.0	38.0	TFTR, JET, JT-60 in late-1980s
Electron temperature, T_e(O) (keV)	6.0	20.0	TFTR, JET, JT-60 in late-1980s
Q_p = fusion power/injected heating power	D–T equivalent $Q_p \simeq 0.25$, using D–D plasmas	3.0	~1 in TFTR, late-1980s, >1 in TFTR and JET, early-1990s
MHD stability	Acceptable only at $q_a > 3$, with $\langle\beta\rangle \lesssim 0.02$	Elimination of major current disruptions	All experiments in large tokamaks in 1980s
Microinstability	Apparently limits T_e and possibly β	Acceptable if no deterioration at higher T_e, T_i, or β	Experiments in TFTR, JET, and D-III Upgrade in mid- and late-1980s
Long-pulse operation Noninductive current drive	Definitive RF demonstrated at low n_e. Neutral beam demonstrations in TFTR	$I_p/P_B = 0.05$ A/W at above T_e, T_i, and β	TFTR and JET in late-1980s (10-s pulses)
Particle and impurity control (including fusion α removal)	Demonstrated for short pulses (~1 s)	Steady-state control of n_e and $Z_{eff} < 2$	JT-60 and ASDEX divertor experiments in mid-1980s (10 s); TFTR and JET in late-1980s (20-s pulses) but at lower power loading

[a] $\bar{n}_e\tau_E = 5\times10^{13}$ cm^{-3} has been achieved at $T_e \simeq T_i$ V 1.5 keV $\langle\beta\rangle \simeq 0.10$).

radius of the reactor will be increased by 0.5 m, and maintenance of the OH primary will be extremely difficult. Alternatively, the throat of the TF coils can be increased by about 1 m in radius and the OH coil can be retained in that position. Either approach will significantly increase reactor cost.

2. The lifetimes of reactor components will be reduced because of thermal fatigue due to pulsing (~ 20,000 pulses/year).
3. Annual neutron production will be reduced approximately 10%. Failure to achieve steady-state current drive is estimated to increase the production cost per fusion neutron by 25–30%.

3.3.3. Need for Additional Technology Development Programs

Because of the unsatisfied technology requirements listed in Table XIV, new programs or significant upgrades of present programs funded by DOE/OFE are needed to expedite the development of TORFA-D2 and other practical tokamak neutron generators. These new or upgraded programs are listed below in order of priority.

3.3.3.1. Steady-State Negative-Ion-Based Neutral Beam. A program that would eventually achieve the beam parameters required for TORFA-D2 is being carried out in a joint Toshiba/Jaeri project in Japan. Operation of a prototype 250-keV, 100-A beam with

Table XIV. Fusion Technology Development Requirements for the TORFA-D2 Fusion Driver

Technology area	Required performance	Existing development programs
Negative-ion-based neutral beam injectors	(1) 100-A ion sources (2) Steady-state operation (3) Overall efficiency of $\geq$ 50%	(1) Ion source and accelerator at LBL and Toshiba (Japan). Required performance expected by 1990. (2) Photodetachment neutralizer at TRW. Required performance expected in late-1980s
Electron-cyclotron heating-power sources	(1) 93 GHz (2) 200 kW per source (3) Pulse length = 1 s (4) Efficiency $\geq$ 20%	Hughes and Varian are developing 60-GHz gyrotrons with the required properties by 1984 and 93-GHz gyrotrons by the late-1980s
Pellet injectors	(1) 3-mm diam (2) v = 3000 m/s (3) tritium pellets (4) 3 pellets/s per injection	ORNL injectors meet size and velocity requirements at low repetition rate. Tritium pellet injector on TFTR expected in late-1980s, and high-repetition rate expected in late-1980s
Disposal of plasma thermal flux	(1) 70 W/cm^2 at first wall, steady state (2) 1 kW/cm^2 on divertor plates, steady state	Ex-reactor test stands in ANL first-wall, blanket/shield program (DOE/OFE), early- to mid-1980s. TFTR, JET, and JT-60 10-s tests in late-1980s
Superconducting magnets	19-mm diameter ring coil, 10 MAT, 5 T (for equilibrium field)	Programs at LANL, ANL, and Westinghouse have been terminated. New programs are required.
Copper magnets	(1) High-strength copper plate, 6 cm thick, 3 m in length (2) demountable joints	(1) A fabrication program is required to demonstrate the feasibility of the copper plate. (2) The demountable joints are similar to D-III coil joints, but a development program is needed to reduce their complexity
Radiation-resistant insulation	(1) Withstands 10^{12} rad (2) Tolerates high stress	A development program is required to adapt candidate insulators such as SPINEL into a suitable form for TF coils
Tritium handling	Throughput = 500 kCi/h	TSTA program at LANL
Remote-maintenance systems	Maintenance and replacement of most reactor components	Modest development programs for TFTR and JET. Significant development programs must be initiated, especially for maintenance of plasma-vessel sector joints and ancillary components.

acceptable current density ($J \simeq 0.05$ A/cm^2) is expected by the early 1990s.

3.3.3.2. Remote-Maintenance Techniques and Equipment. The U.S. program in this area is almost nonexistent. A program funded at $10 million or more per annum is needed to develop and prove practical remote-maintenance techniques and specialized equipment for tokamak reactor use. This program would make use of full-sized mockups of FED-R sectors.

3.3.3.3. Magnet Coil Demountable Joints. A new development program is needed to identify, test, and prove out joints for TF and PF coils that are less complex than joints now in use and that are acceptable for high-field coils.

3.3.3.4. Radiation-Resistant Coil Insulation. SPINEL ($MgAl_2O_4$) has been identified as the most promising of present insulators. A development program is needed to characterize it mechanically and to proof-test it onto the plates that comprise the TF

coils. A different form of SPINEL is required for use in wound copper PF coils.

3.3.3.5. Superconducting Ring Coils. The DOE/OFE program for developing pulsed NbTi coils with up to 1 GJ of stored energy and up to 7-T magnetic fields must be reactivated so that the external PF coils of near-term tokamak test reactors can be superconducting.

3.4. Conversion of the FED-R Facility to TORFA-D2

The FED-R concept design project envisages a two-stage operating program for the FED-R test reactor. Although Stage-II specifications call for higher magnetic field, plasma, and neutral beam power, the tokamak configuration is unchanged. However, the ability to modify the TF coils of FED-R permits relatively inexpensive conversion of the test reactor to a production reactor of at least 250 MW fusion power, or about 60% that of TORFA-D2. Conversion would be accomplished as follows:

1. The TF coil joints would be disassembled, and all the outboard legs would be retracted.
2. Segments of 1 m in length would be inserted in the top and bottom arms. The innermost end of each segment would be permanently joined to the stationary section of each coil.
3. The FED-R vacuum vessel would be replaced by a vessel with a larger major radius.
4. The TORFA-D2 blanket assemblies would be installed around the new vacuum vessel (e.g., the 40 cm of inboard shielding would be replaced by 80 cm of blanket/shield).
5. When the outboard TF coil legs are rejoined to the stationary sections, the horizontal bore of the coils would increase approximately 1 m. The increase in TF-coil power dissipation would be 5% for a given magnetic field at the conductor.
6. The internal PF coils would be retained, but their currents would be reprogrammed. The plasma current would be the same as in FED-R (4.4 MA maximum for Stage II).
7. The external PF coils could be retained if, initially, they were a little oversized for the FED-R Stage I.
8. The 150-keV neutral beam injectors would be upgraded to 250 keV, as is planned for Stage II.
9. Additional modules (as necessary for FED-R Stage I) would be provided for power supplies and coolant systems. All other machine and facility subsystems would be essentially unchanged.

The fusion power after conversion would be closer to the 560 MW specified for TORFA-D2 if, originally, the TF coils had been designed for a somewhat higher field ($B_M = 9.8$ rather than 8.8 T) and the PF coils had been designed for a somewhat higher current (5.0 rather than 4.4 MA).

If conversion of FED-R into a production reactor were anticipated during the FED-R design phase, the siting of the FED-R facility would be selected accordingly.

Table XV outlines a schedule for implementing TORFA-D2; this outline is based on the assumption that a vigorous program is needed. Based on the performance of the TFTR and other large tokamaks

Table XV. Implementation Schedule for a Tokamak Test Reactor (FED-R) That Can Be Converted into a Materials Production Reactor (TORFA-D2)

Period of task	Activity
Conceptual design	1981–1984
Preliminary engineering design	1984–1986
Critical design decisions	
Steady-state current drive	1985
Magnetic divertor configuration	1985
Required magnetic field strength[a]	1985
Final engineering design	1986–1988
Fabrication and assembly	1988–1992
Integrated machine and plasma systems checkout	1992–1994
Testing of prototype blanket systems	1994–1997
Conversion of FED-R into TORFA-D2	1997–1999
Modification of TF coils	
Replacement of vacuum vessel	—
Upgrading of natural beam injectors	—
Operation of production reactor	1999–2030

[a] TORFA-D2 requires a B_M of 9.8 T, while FED-R requires a maximum B_M of 8.8 T.

in the mid-1980s, as well as on the progress in fusion technology development, there is still adequate opportunity to establish checkpoints so that major uncertainties in vital design options can be resolved before the final engineering design is started. These options include (1) the possibility of specifying a very small OH transformer given a high degree of viability of noninductive current drive, (2) the optimal configuration of the magnetic divertor to be used for heat removal and particle control, and (3) the strength of the magnetic field required on the basis of attainable beta values.

4. COMPARISON OF TANDEM MIRROR AND TOKAMAK FUSION DRIVERS

4.1. Common Fusion Technologies

Although the tokamak and tandem mirror are markedly different devices (cf. Fig. 1), many of their component technologies are similar and in some cases virtually identical. In this section we point out the major subsystems that are essentially the same and can therefore, enjoy all-out development without the prior choice of a fusion driver for a production reactor. These subsystems have been discussed in some detail in Sections 1. and 2.

4.1.1. Negative-Ion-Based Neutral Beams

Both the TMPR and tokamak require the use of D^-- and T^--based neutral beams of the type now being developed at LBL. These injectors will use a surface-conversion negative-ion source coupled to a TFF electrostatic accelerator. The energetic ion beam is then neutralized with a photodetachment neutralizer. The various beam energies required by the TMPR and the tokamak are in the 200- to 500-keV range and can be produced efficiently with this type of injector.

4.1.2. ECH Power Sources

The 100-GHz, 200-kW long-pulse gyrotrons being developed by the DOE/OFE are required in both the TMPR and tokamak. The TMPR also needs a variable-frequency millimeter wave source, such as the free-electron laser.

4.1.3. Pellet Injectors

The DOE/OFE is currently developing pellet injectors that will accelerate 1- to 5-mm-diam cryogenic pellets to speed up to 3×10^5 cm/s. The same injectors are specified for fueling the TMPR central cell and the tokamak plasma.

4.1.4. Radiation-Resistant Insulation

The TMPR requires radiation-resistant insulation (i.e., lifetime of 10^{12} rad) for the copper magnet inserts in the end plugs, where the neutron flux is low but the magnets are unshielded. The tokamak requires similar insulation in the copper toroidal-field coils; although these are shielded, the fusion neutron flux is large. While promising candidate insulators such as SPINEL have been identified, a materials development program is needed for application to copper magnets.

4.1.5. Tritium-Handling Systems

Once the tritium is released from the cryopumps in the TMPR vacuum vessel, the pumping processes are the same as those in the tokamak. The external tritium-handling systems, including gettering, purification, and reinjection as pellets or by neutral beam injectors, as well as the tritium cleanup systems in the reactor cell, have similar capacities for each fusion driver and nearly identical features.

4.2. Comparative Status of Plasma Physics

The abbreviation MFPR is used in the following paragraphs to denote magnetic fusion production reactor, with no distinction being made between mirror and tokamak machines.

4.2.1. β

The mirror machine has, essentially, achieved the β required for an MFPR, but only for very short pulses (~ 10 ms) and low temperatures. The tokamak has achieved β values that are about a factor of 2 smaller than those required for an MFPR, but only at low values of T_e and T_i.

4.2.2. Confinement Parameter

The $n_e\tau_E$ required for the TMPR is a factor of 5 to 10 larger than that required for the TPR. The reason is that the central-cell plasma of the mirror must be close to thermonuclear ignition to generate significant wall loading at moderate beam powers in the end plugs, thereby giving moderately high Q_p. The TPR, on the other hand, can make use of beam-target reactions in the torus and can, both by beam fueling and direct beam heating of the bulk ions, maintain a high T_i even at relatively low $n_e\tau_E$. The best $n_e\tau_E$ achieved in mirrors is 4 orders of magnitude smaller than required for a MFPR. It is in this area that the extrapolation from present-day mirror-machine performance is most speculative. The required $n\tau_E$ has actually been reached in *low-temperature*, low-β operation in tokamaks. However, the best $n\tau_E$ achieved at high temperature is still a factor of 6 smaller than that required.

4.2.3. Ion Temperature

The mirror machine requires a several-hundred-factor increase in T_i in the central cell, while the tokamak requires only a factor-of-4 increase.

4.2.4. Electron Temperature

The mirror requires a factor-of-600 increase in T_e while the tokamak requires only a factor-of-4 increase.

4.2.5. Plasma Q Value

Heretofore the ion temperature in the central cell of tandem mirrors has been too small for measurable neutron production. The largest D–T-equivalent Q_p achieved in tokamaks (TFTR) is a factor of 12 smaller than required.

4.2.6. MHD Stability

To date, mirror-machine experiments have revealed no MHD stability problem. Tokamak experiments reveal serious problems under the conditions required to achieve high β, and major plasma disruptions still cannot be eliminated.

4.2.7. Microinstability

Microinstabilities observed in mirror-machine experiments may limit the confinement times in future machines. Microinstabilities observed in tokamaks may limit T_e and possibly β in future machines. In both cases the result may be a lower Q_p than required.

4.2.8. Long-Pulse or Steady-State Operation

Mechanisms for removing fusion α particles from both mirrors and tokamaks are unproved. Impurity concentrations have been kept to satisfactory levels in both mirror-machine and tokamak experiments. Steady-state tokamak operation depends on an effective method of noninductive current drive, which, to date, has only been demonstrated at densities five times lower than those required for an MFPR.

4.2.9. Summary

Mirror machines have, essentially, already achieved the β and MHD stability properties necessary for an MFPR, while achieving the satisfactory β and MHD performance of tokamak plasmas is still in doubt. The ability to attain steady-state operation is less problematical for mirror machines. However, the plasma temperatures and confinement parameters already achieved by tokamaks are orders of magnitude closer than the present-day tandem-mirror parameters to the values needed in an MFPR.

4.3. Present Status and Development Requirements of Fusion Technologies

4.3.1. Neutral Beam Injectors

The TMPR requires a modest upgrade of present-day, positive-ion-based neutral beam injectors while the TPR needs no positive ion beams. Both the TMPR and TPR require negative-ion-based beams, now in a rudimentary development stage. The TMPR specifies a beam current that is an order of magnitude higher than that for the TPR, which results in more demanding beam optics in order to inject through minimal-sized ports (and conserve breeding blanket space). The TPR requires a somewhat higher beam energy.

4.3.2. ECRH

The TPR requirements will be met by the present DOE development program. If the TMPR requires a *tunable* high-frequency source, a new development program based on the free-electron laser must be pursued.

4.3.3. Pellet Injectors

Present technology is capable of providing the pellet velocities needed for the TPR ($\leqslant 3$ km/s). However, a more advanced pellet-acceleration technology may be needed for the TMPR (possibly up to 10 km/s).

4.3.4. Disposal of Plasma Efflux

DOE/OFE programs are developing the materials needed for steady-state disposal of particle and radiation efflux from tokamak reactor plasmas. Plasma direct conversion from tandem mirrors has been demonstrated at the required efficiency at lower power density. A development program is in place to demonstrate direct conversion at the power densities characteristic of a TMPR.

4.3.5. Superconducting Magnets

The coils required for both the TPR (external ring coils) and the TMPR (excluding Nb_3Sn inserts for the hybrid magnets), have quasi-steady currents and represent modest extrapolations from present-day technology.

4.3.6. Copper Magnets

The feasibility of implementing readily demountable joints in very large TF coils and in the internal PF coils must be demonstrated for the TPR. A demonstration of the long-term reliable operation of layered hybrid coils at fields approaching 20 T is required for the TMPR.

4.3.7. Other Areas

Extrapolations and development requirements for the radiation-resistant insulation, tritium-handling systems, and remote-maintenance systems are similar for the TMPR and TPR. Reference 2 compares remote-maintenance procedures for the TMPR and TPR; in general, TPR procedures are somewhat more difficult.

4.3.8. Summary

Significant technological developments are needed for both the TMPR and TPR. Some of these technologies are similar (see Section 4.1.), while others occur in different areas. Overall, the technological extrapolations for both concepts seem to be comparable.

4.4. Blanket-Coverage Factors

If a fusion-based production reactor is to produce special nuclear materials at a competitive cost, the breeding blanket assemblies must intercept and capture as close to 100% of the fusion neutrons as possible. This objective tends to be subverted in the TMPR by the end-plug regions, which contain no blankets. While the net leakage of fusion neutrons from the central cell into the end plugs is no more than 2% of the total production rate in the central cell, there is a significant D–T reaction in the end plugs producing neutrons that are not absorbed profitably. Thus, a certain percentage of the blanket-generated tritium is consumed for no useful purpose. The result is an effective blanket coverage factor of 94%.

The tokamak's difficult geometry makes it impossible for the breeding blanket assemblies to completely cover the vacuum vessel. Blanket coverage is reduced further by the torus-wall penetrations needed for neutral beam and pellet injection. The hardware in the divertor region at the bottom of the torus also seriously reduces effective coverage. While most of the incident fast neutrons will either penetrate this hardware or be scattered into other regions of the torus, the transmitted or scattered neutrons will have relatively low energies and will be incapable of neutron multiplication in the blankets.

Preliminary estimates[39] indicate, for the blanket configurations developed in this project, that the overall breeding rate per fusion neutron in the tokamak production reactor would be about 7% less than that in the TMPR. After subtracting the tritium required to fuel the reacting plasma, the tokamak generates significantly fewer net atoms per fusion neutron.

5. CONCLUSION

For an MFPR to be built on the basis of either reactor concept, both the tokamak and tandem mirror require comparable advances in fusion-related technologies. On the other hand, the plasma parameters achieved to date in tokamaks are markedly closer to those required in an MFPR than are the parameters achieved in tandem mirrors. Nevertheless, the somewhat higher blanket coverage factor inherent in the tandem mirror, the reduced difficulty in processing the blankets, and the greater assuredness of steady-state operation have encouraged the study of the mirror-machine option.

ACKNOWLEDGMENTS

This work was performed under the auspices of the U.S. Department of Energy by the Lawrence Livermore National Laboratory under contract number W-7405-ENG-48.

REFERENCES

1. D. L. Jassby, Selection of a toroidal fusion reactor concept for a magnetic fusion production reactor, *J. Fusion Energy*, companion paper in this series.
2. W. S. Neef and D. L. Jassby, Mechanical design of a magnetic fusion production reactor, *J. Fusion Energy*, companion paper in this series.
3. G. A. Carlson et al., Comparative end-plug study for tandem mirror reactors, Lawrence Livermore National Laboratory, Livermore, California UCID-19271 (1981).
4. R. W. Moir, Ed., Tandem mirror hybrid reactor design study final report, Lawrence Livermore National Laboratory, Livermore, California UCID-18808 (1980).
5. M. N. Rosenbluth, H. L. Berk, D. E. Baldwin, H. V. Wong, and T. M. Antonsen, Sherwood Theory Meeting, (Santa Fe, New Mexico 1982), paper 3A2.
6. D. E. Baldwin and B. G. Logan, Lawrence Livermore National Laboratory, Livermore, California, private communication.
7. Mirror advanced reactor study (MARS) interim design report, Lawrence Livermore National Laboratory, Livermore, California UCRL-53333 (1982).
8. S. A. Freije et al., Impact of gyrotron characteristics on a mirror reactor (to be published in Int. Electronics).
9. Celilo-northern terminal-pacific HVDC intertrie, U.S. Department of the Interior and Bonneville Power Administration (1970).
10. F. C. Beriger et al., Cabora Basa HVDC transmission: Oil-cooled outdoor thyristor values, *IEEE PES Summer Meeting of the Energy Research Conference*, (Anaheim, California, 1974), T 74, 459–4.
11. HVDA and ASEA specialty, ASEA Pamphlet KS10–100 E.
12. M. Loring, The OFE/ORNL national gyrotron development program, Gyrotron User/Developer Meeting, Germantown, Maryland, 1982 (U.S. DOE Office of Fusion Energy, Germantown, Maryland, 1982), p. 170.
13. Discussions with Marshall Loring.
14. M. Read, NRL multimegawatt program, Gyrotron User/Developer Meeting, Germantown, Maryland, 1982 (U.S. DOE Office of Fusion Energy, Germantown, Maryland, 1982), p. 170.
15. G. Goubau and F. Schwering, On the guided propagation of electromagnetic wave beams, *IRE Trans. Antenn. Propag.* **AP-9**:248 (1961).
16. R. J. Caffin and J. B. Boyer, A low loss launcher for the beam waveguide for millimeter waves, *IEEE Trans. Microwave Theory Tech.* **MIT-12**(9):555 (1964).
17. J. N. Hines et al., The electrical characteristics of the conical horn-reflector antenna, *Bell Syst. Tech. J.* **7**:1187 (1963).
18. C. P. Moeller, Status of components for the COUBLETT III and PDX ECRH experiments, Gyrotron User/Developer Meeting, Germantown, Maryland, 1982 (U.S. DOE Office of Fusion Energy, Germantown, Maryland, 1982), p. 85.
19. P. D. Potter, A new horn antenna with suppressed sidelobes and equal beamwidths, *Microwave J.* **6**:71 (1963).
20. J. B. Beyer and E. H. Scheibe, Higher modes in guided electromagnetic beams, *IRE Trans. Antenn. Propag.* **AP-10**:349 (1963).
21. G. H. Neilson et al., Injection-dominated tokamak experiments at ORNL, *Joint Vareena-Grenoble International Symposium Heating Toroidal Plasmas* (Grenoble, France, 1978), p. 49.
22. H. Eubank et al., PLT neutral beam heating results, Proceedings of the 7th Conference Plasma Physics and Controlled Nuclear Fusion Research, Brussels, Innsbruck, 1978 (IAEA, 1978), IAEA-CN-37/C-3, p. 167.
23. M. Murakami et al., Neutral beam experiments in the ISX-B tokamak, Proceedings of the 8th Conference on Plasma Physics and Controlled Nuclear Fusion Research, Brussels, Innsbruck, 1978 (IAEA, 1978), IAEA-CN-38/N-1, p. 377.
24. K. H. Berkner et al., Performance characteristics of NBSTF, the prototype neutral beamline for TFTR, Proceedings of the 9th Symposium on Engineering Problems in Fusion Research (Chicago, Illinois, 1981), p. 763.
25. A. Deitz et al., The TFTR neutral beam power system, Proceedings of the 7th Symposium on Engineering Problems in Fusion Research (Knoxville, Tennessee, 1977), p. 1151.
26. K. N. Leung and K. W. Ehlers, Self-extraction negative ion source, *Rev. Sci. Instrum.* **53**:803 (1982).
27. W. K. Dagenhart et al., Proceedings of the 2nd International Symposium Prod. Neutral. Negative Ions and Beams, Brookhaven National Laboratory, BNL-53104 (1980).
28. K. Prelec et al., Proceedings of the 3rd Workshop on Development of Neutral Beam Injectors, Gatlinburg, Tennessee, 1981.
29. K. W. Berkner et al., *Nucl. Fus.* **15**:249 (1975).
30. G. I. Dimov et al., *Sov. Phys. Tech. Phys.* **22**(9), 1091 (1977).
31. FED-R, A fusion engineering device utilizing resistive magnets, Fusion Engineering Design Center, Oak Ridge, Tennessee ORNL/FEDC-82/1 (1982).
32. D. L. Jassby, TORFA—Toroidal reactor for fusion applications, Princeton Plasma Physics Laboratory, Princeton, New Jersey, PPPL reports March and May 1980 and PPPL-1700 (1980). Also see J. Kalnavarns and D. L. Jassby, Resistive toroidal field coils for tokamak reactors, Princeton Plasma Physics Laboratory, Princeton, New Jersey PPPL-1685 (1980).
33. D. J. Grove, The status of TFTR, *Proceedings of the 4th Topical Meeting on Technical Controlled Fusion* (U.S. Department of Energy, 1981), CONF-801011, p. 957–961.

34. D. R. Mikkelsen and C. E. Singer, Optimization of steady-state beam-driven tokamak reactors, Princeton Plasma Physics Laboratory, Princeton, New Jersey, PPPL-1929 (1982), and associated references.
35. Proceedings of the 9th International Conference Plasma Physics on Controlled Nuclear Fusion Research, Baltimore, Maryland, 1982, papers R-1, R-2, and R-4. Also see R. J. Fonck et al., *J. Nucl. Mat.* **111**:343–354 (1982).
36. Maintenance concepts, Ref. 31, Chap. 9.
37. G. F. Hurley et al., *J. Nucl. Matls.* **103**:761–765 (1981).
38. Impurity control and first-wall engineering, in *U.S. FED/INTOR Critical Issues* (1982), Vol. 1, Chap. 7.
39. J. D. Lee, Nuclear fusion production reactor, *J. Fusion Energy*, companion paper in this issue.